Journal of Steroid Biochemistry and Molecular Biology 231 (2023) 106315

Contents lists available at ScienceDirect

Journal of Steroid Biochemistry and Molecular Biology

journal homepage: www.elsevier.com/locate/jsbmb

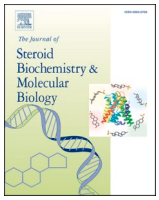

Dihydrotestosterone-based A-ring-fused pyridines: Microwave-assisted synthesis and biological evaluation in prostate cancer cells compared to structurally related quinolines

Márton A. Kiss [a], Miroslav Peřina [b], Laura Bereczki [c,d], Ádám Baji [a], Jakub Bělíček [b], Radek Jorda [b,*], Éva Frank [a,*]

[a] Department of Organic Chemistry, University of Szeged, Dóm tér 8, H-6720 Szeged, Hungary
[b] Department of Experimental Biology, Faculty of Science, Palacký University Olomouc, Šlechtitelů 27, 78371 Olomouc, Czech Republic
[c] Structural Research Centre, Research Centre for Natural Sciences, Magyar tudósok körútja 2, H-1117 Budapest, Hungary
[d] Institute of Materials and Environmental Chemistry, Research Centre for Natural Sciences, Magyar tudósok körútja 2, H-1117 Budapest, Hungary

ARTICLE INFO

Keywords:
Dihydrotestosterone
Pyridines
Androgen receptor
Crystal structure
Transcriptional activity

ABSTRACT

Dysfunction of the androgen receptor (AR) signalling axis plays a pivotal role in the development and progression of prostate cancer (PCa). Steroidal and non-steroidal AR antagonists can significantly improve the survival of PCa patients by blocking the action of the endogenous ligand through binding to the hormone receptor and preventing its activation. Herein, we report two synthetic strategies, each utilizing the advantages of microwave irradiation, to modify the A-ring of natural androgen 5α-dihydrotestosterone (DHT) with pyridine scaffolds. Treatment of DHT with appropriate Mannich salts led to 1,5-diketones, which were then converted with hydroxylamine to A-ring-fused 6′-substituted pyridines. To extend the compound library with 4′,6′-disubstituted analogues, 2-arylidene derivatives of DHT were subjected to ring closure reactions according to the Kröhnke's pyridine synthesis. The crystal structure of a monosubstituted pyridine product was determined by single crystal X-ray diffraction. AR transcriptional activity in a reporter cell line was investigated for all novel A-ring-fused pyridines and a number of previously synthesized DHT-based quinolines were included to the biological study to obtain information about the structure-activity relationship. It was shown that several A-ring-fused quinolines acted as AR antagonists, in comparison with the dual or agonist character of the majority of A-ring-fused pyridines. Derivative **1d** (A-ring-fused 6′-methoxyquinoline) was studied in detail and showed to be a low-micromolar AR antagonist (IC_{50} = 10.5 μM), and it suppressed the viability and proliferation of AR-positive PCa cell lines. Moreover, the candidate compound blocked the AR downstream signalling, induced moderate cell-cycle arrest and showed to bind recombinant AR and to target AR in cells. The binding mode and crucial interactions were described using molecular modelling.

1. Introduction

The androgen receptor is a ligand-activated transcription factor from the family of steroid hormone receptors, which plays a fundamental role in the normal development and physiology of male tissues. Upon binding of androgens, AR undergoes substantial conformational changes, various post-translation modifications, and is imported into nucleus where it interacts with co-regulators and DNA and modulates its transcriptional program [1].

Overexpression of AR, which might be accompanied by the relaxation of its regulation is strongly connected with the development of prostate cancer (PCa), which is the second most common cancer in men (USA). First-line therapy targets androgen biosynthesis to decrease the level of plasma-circulating androgens (by orchiectomy, modulation of the luteinizing hormone release or CYP17A1 inhibitors). Androgen-deprivation therapy is usually combined with the AR antagonists, to block the pro-oncogenic signalling. Several steroidal (abiraterone, galeterone) or non-steroidal antagonists (e.g., enzalutamide, apalutamide, darolutamide, rezvilutamide) (Fig. 1) have entered clinical trials or were successfully approved as drugs [2]. Despite being very effective

* Corresponding authors.
E-mail addresses: radek.jorda@upol.cz (R. Jorda), frank@chem.u-szeged.hu (É. Frank).

https://doi.org/10.1016/j.jsbmb.2023.106315
Received 7 March 2023; Received in revised form 19 April 2023; Accepted 20 April 2023
Available online 21 April 2023

and demonstrating an overall survival benefit in the castration-sensitive state, the treatment frequently progresses into the castration-resistant PCa (CRPC) stage characterized by further alterations in AR signalling and undruggable splicing variants. Although various anti-AR strategies have been introduced (targeting the transcription of the AR gene, stability of transcript or protein, intracellular trafficking of AR or its downstream signalling [3–5]), still a number of AR-related mechanisms of resistance exist and novel strategies are needed to overcome them.

Pyridine-based ring systems, including quinolines comprising benzene-fused pyridines, are among the most prevalent structural motifs in drug design, with numerous bioactive representatives already identified [6–9]. The best-known steroidal pyridine derivative, abiraterone (Fig. 1), used as its acetate prodrug in the treatment of castration-resistant PCa, inhibits the CYP17A1 enzyme involved in androgen biosynthesis, thus preventing testosterone production in the adrenal glands and intratumorally [10]. Besides reduced hormone levels, abiraterone is also able to bind directly to the AR and block its activity as a ligand-dependent transcription factor [11]. Other D-ring--modified steroidal pyridines, structurally similar to abiraterone, were also investigated and found to be effective *in vitro* against androgen-sensitive and -insensitive prostate cancer cell lines (LNCaP and PC-3) [12]. Moreover, some D-ring-condensed [13] and D-secosteroid-connected quinolines [14] were also found to be effective anticancer agents. In contrast, steroids fused with a pyridine or quinoline moiety in the A-ring are less studied and only a few examples have been reported but without biological supplementation [15].

We have previously demonstrated that introducing different N-containing heterocycles to the A-ring of DHT can result in compounds that reduce the transcriptional activity of AR and exhibit antiproliferative activity in AR-positive PCa cell lines [16,17]. As our goal – in the absence of an AR crystal structure in antagonistic conformation [18] – is to investigate systematically the effect of additional heterorings condensed to the A-ring of DHT on biological activity, in this article we report the synthesis and biological evaluation of novel mono- and disubstituted pyridine-fused derivatives (series **2** and **3**, Fig. 2). All new compounds were structurally characterized by ^{1}H and ^{13}C NMR spectroscopy and electrospray ionization mass spectrometry (ESI-MS), and in the case of a representative novel pyridine derivative, by single crystal X-ray diffraction. A number of steroidal A-ring-fused quinolines (**1a**–**i**, Fig. 2) that have displayed modest antiproliferative activity against a panel of human gynaecological malignant cell lines [19], but have not previously been investigated for their effects on AR signalling, were also included in the current biological study due to structural similarity. Accordingly, the DHT-based quinolines and the newly prepared

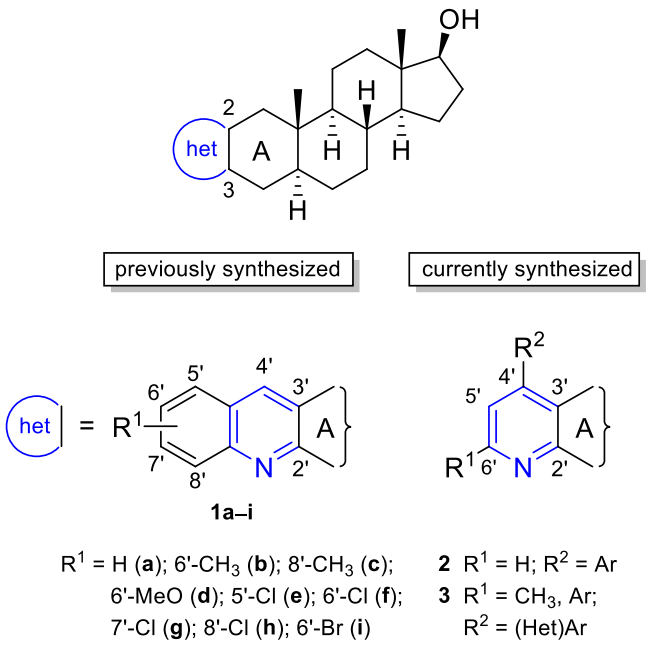

Fig. 2. Steroidal A-ring-fused quinolines [19] and pyridines investigated in this study.

pyridines were primarily screened for their ability to affect the transcriptional activity of AR in a reporter cell line. Candidate compound **1d** was further studied and showed to be a low-micromolar AR antagonist, it suppressed the viability and proliferation of AR-positive PCa cell lines. Moreover, the candidate compound blocked the AR downstream signalling, mainly in wild-type AR model, induced moderate G1 arrest and was proven to bind the AR in cells and the recombinant AR protein as well. The binding mode and interaction was described using molecular modelling.

2. Results and discussion

2.1. Synthesis and characterization of DHT-based pyridine derivatives

As a first synthetic step, the regioselective modification of the A-ring of DHT was planned to be carried out using 3-(dimethylamino)propiophenone hydrochloride (**4a**) leading to a 1,5-diketone moiety at C-2 position. By amine elimination, β-amino ketone hydrochloride salts are

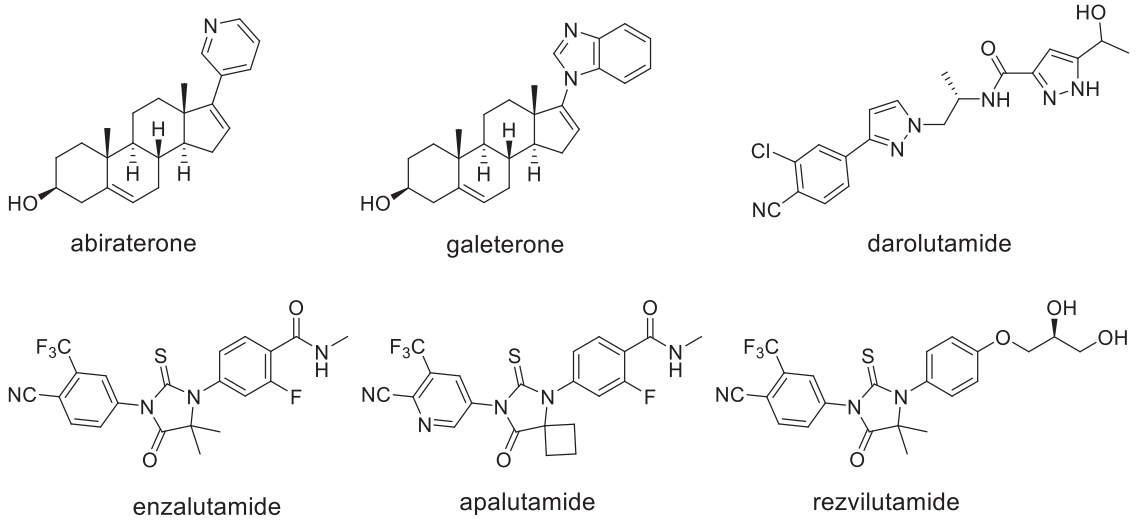

Fig. 1. Examples of different types of antiandrogens.

Table 1
Synthesis of DHT-derived A-ring-fused 6'-substituted pyridine derivatives.

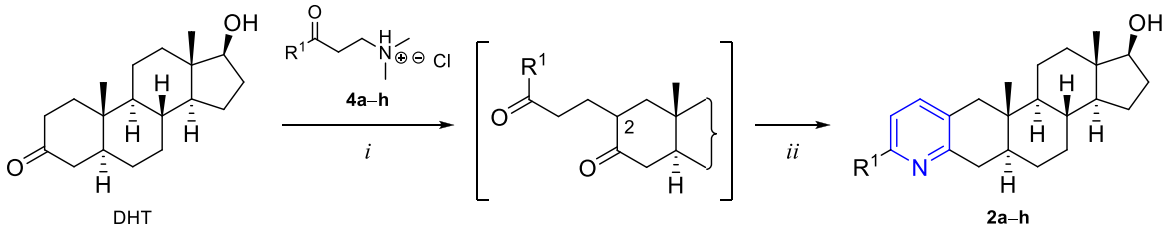

Entry	R^1	Product[a]	Yield (%)[b]
1	Ph	**2a**	81
2	*p*-CH_3-C_6H_4	**2b**	70
3	*p*-MeO-C_6H_4	**2c**	79
4	*p*-NO_2-C_6H_4	**2d**	72
5	*p*-F-C_6H_4	**2e**	80
6	*p*-Cl-C_6H_4	**2f**	72
7	*p*-Br-C_6H_4	**2g**	78
8	*o*-OH-C_6H_4	**2h**	67

Reagents and conditions: *i*) pyrrolidine, 1,4-dioxane, 120 °C, 20 min, MW; *ii*) $HONH_2$·HCl, EtOH, 90 °C, 10 min, MW.
[a] Heterocyclization was performed with the crude diketone intermediate.
[b] Calculated for two steps from DHT after column chromatography.

able to form α,β-unsaturated ketones *in situ* [20], which can act as Michael acceptors in the reaction with DHT. Preliminary experiments under conventional heating in absolute EtOH, using triethylamine (TEA) as a base, showed the formation of a new product, but complete conversion was not achieved even after 24 h. In order to facilitate the alkylation reaction, pyrrolidine was applied instead of TEA in 1, 4-dioxane to generate the corresponding enamine *in situ* from DHT, which then readily reacted as a more efficient Michael donor under microwave (MW) conditions with **4a** according to the Stork enamine alkylation [21]. After 20 min of irradiation, only a small amount of residual starting material and a spot of a newly formed compound with a similar retention factor were detected by thin-layer chromatography (TLC). The crude product was used in the heterocyclization reaction without further purification (Table 1, entry 1).

Our initial attempts for a tandem-like cyclization of the dicarbonyl intermediate with hydroxylamine hydrochloride as an ammonia surrogate [22] in the previously used 1,4-dioxane led to incomplete conversion and the formation of a dioxime product verified by ESI-MS. In contrast, the desired 6'-phenylpyridine derivative **2a** was successfully obtained when the dioxane was evaporated and the residue was redissolved in absolute EtOH. Compound **2a** was purified by column chromatography on silica gel, but high yields were only obtained when dichloromethane containing 1 v/v% TEA was used as eluent. To extend the compound library, Mannich salts **4b**–**h** from various substituted aryl-methyl-ketones were synthesized according to methods described previously [23,24]. These were then all subjected to 1,5-diketone formation from DHT, followed by cyclization to obtain the corresponding 6'-monosubstituted A-ring-condensed pyridines (**2b**–**h**) in moderate to good yields, regardless of the electronic nature of the R^1 substituent (Table 1, entries 2–8).

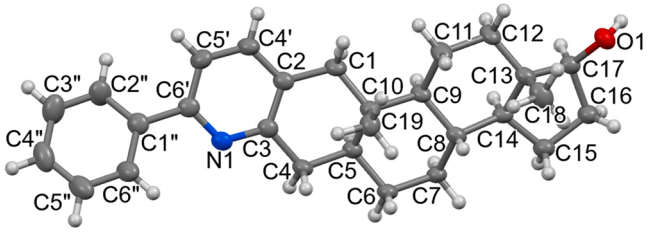

Fig. 3. Molecular model and atom labelling of **2a**. Ellipsoid representation, displacement parameters are drawn at the 50% probability level.

The solid phase structure of a colourless prism of **2a** was determined by single crystal X-ray diffraction (Fig. 3). The molecule crystallized in the monoclinic crystal system, in $P2_1$ space group. The asymmetric unit contains two molecules in the opposite position and the unit cell contains four molecules.

The configuration of **2a** is established based on the known absolute configuration of the utilized natural starting compound, R at C8 and C8 * and S at C5, C5 * , C9, C9 * , C10, C10 * , C13, C13 * , C14, C14 * , C17, C17 * (Fig. S1). Molecules of **2a** are arranged parallel to each other in columns running along the *b* crystallographic axis (Fig. 4). C-H…π interactions stabilize the packing (Fig. S2). In the molecule of **2a**, only one acceptor (N1, N1') and one donor atom are present (O1, O1') and a hydrogen bond is formed between them that connects the columns formed by the stacking of the molecules. Additionally, the O1 oxygen accepts a hydrogen from a carbon donor (Table S1).

As a continuation, similar analogues substituted at both C-4' and C-6' positions of the pyridine moiety were aimed to be synthesized. For this, steroidal arylidene derivatives **5a**–**e**, previously obtained from DHT [16, 17,25] were used as starting materials, since these α,β-enones can be reacted with α-pyridinium methyl ketone salts in Kröhnke pyridine cyclization reactions. Thus, 1-(2-oxo-phenylethyl)pyridinium iodide (**6a**) and its analogues (**6b**, **6c**) were first prepared in an Ortoleva-King reaction by heating acetophenone, 2'-hydroxyacetophenone or 2-acetylpyridine with elemental iodine in pyridine according to the method described in the literature [26,27]. The resulting precipitates were washed with cold pyridine and diethyl ether several times, and the crude products were used in the following cyclization of **5a**–**e** with ammonium acetate under Kröhnke conditions (Table 2). Systematic combination of **5a**–**e** with **6a**–**c** in the pyridine formation reactions resulted in 15 differently substituted heterocyclic products **3a**–**o** in moderate to good yields (51–82%) after chromatographic purification.

The structure of all novel products was confirmed by NMR spectroscopy and ESI-MS measurements. The characteristic splitting of 1-H_2 (two doublets) and 4-H_2 (two double doublets) in the ^{1}H NMR spectra is indicative for the 2,3-fused heteroring. The signals of protons at C4' and C5' of the pyridine ring in **2a**–**g** can be detected as doublets with the same coupling constant of around 8 Hz. However, only a singlet proton peak (5'-H) can be noticed for the highly substituted pyridine ring of **3a**–**o**.

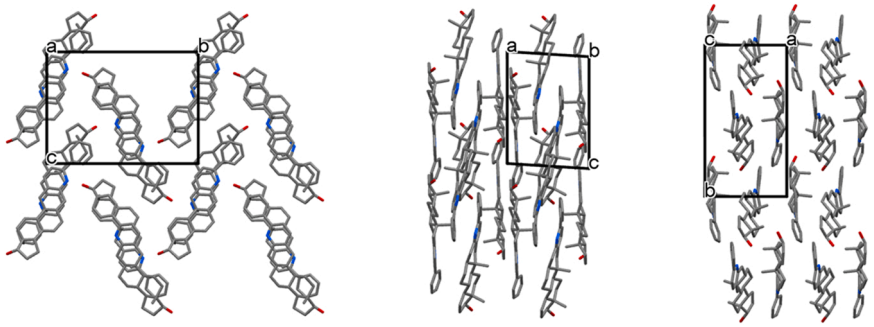

Fig. 4. Crystal packing of **2a** shown in the *a*, *b* and *c* crystallographic directions. Molecules are drawn by stick representation, hydrogens are omitted for clarity.

Table 2
Synthesis of DHT-derived A-ring-fused 4',6'-disubstituted pyridine derivatives.

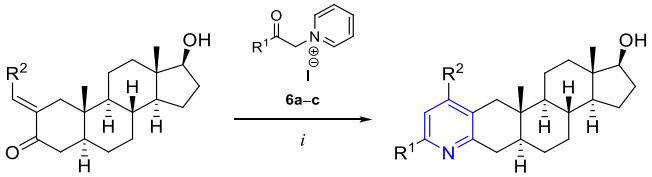

Entry	Enone	R^2	R^1	Product	Yield (%)
1	**5a**	CH_3	Ph	**3a**	72
2			*o*-OH-C_6H_4	**3b**	65
3			pyridin-2-yl	**3c**	71
4	**5b**	Ph	Ph	**3d**	77
5			*o*-OH-C_6H_4	**3e**	76
6			pyridin-2-yl	**3f**	82
7	**5c**	*p*-F-C_6H_4	Ph	**3g**	67
8			*o*-OH-C_6H_4	**3h**	59
9			pyridin-2-yl	**3i**	68
10	**5d**	*p*-Cl-C_6H_4	Ph	**3j**	73
11			*o*-OH-C_6H_4	**3k**	70
12			pyridin-2-yl	**3l**	77
13	**5e**	*p*-Br-C_6H_4	Ph	**3m**	52
14			*o*-OH-C_6H_4	**3n**	51
15			pyridin-2-yl	**3o**	54

Reagents and conditions: *i*) NH_4OAc, EtOH, MW, 90 °C, 20 min.

2.2. Screening of compounds for their activity towards AR and PCa cells' viability

We recently reported several DHT-based A-ring-fused (hetero)arylidenes, azolo[1,5-*a*]pyrimidines, and differently substituted pyrazoles and their targeting of the AR in PCa cell lines [16,17].

In this study, novel DHT derivatives by modifying the A-ring with mono- and disubstituted pyridines (**2a**–**h** and **3a**–**o**) are introduced. These series were extended with some structurally similar quinolines (**1a**–**i**, Fig. 2), which were previously published but were not pharmacologically investigated in relation to AR.

Transcription of AR-regulated genes is tightly connected to its activity, as AR is a direct transcription factor. Therefore, inhibition of transcriptional activity was evaluated at first using AR-dependent reporter cell line (22Rv1-ARE14), expressing the inserted luciferase gene under the control of AR-response element [28]. All compounds were screened to their effect on AR transcriptional activity at three concentrations (2 – 10 – 50 μM) in both agonist (evaluation of the ability to induce the AR activation in comparison to the synthetic agonist R1881) and antagonist mode (evaluation of the ability to suppress the AR activation in the presence of synthetic agonist R1881).

The analysed library comprised 9 already published steroidal A-ring-fused quinolines (**1a**–**1i**) [19], 8 novel A-ring-fused 6'-substituted pyridine derivatives (**2a**–**2h**) and 15 A-ring-fused 4',6'-disubstituted pyridine derivatives (**3a**–**3o**). From the 32 evaluated compounds, 14 were able to decrease the AR-transcriptional activity in the antagonist scheme of the experiment in 50 μM. Overall, A-ring-fused quinoline derivatives were the most potent derivatives (Table 3), from which 3 compounds (**1a**, **1d**, **1i**) were able to diminish the R1881-activated AR transcriptional activity to approx. 50% at 10 μM concentration. Based on the structure comparison, the potent derivatives were unsubstituted A-ring fused quinoline (**1a**) or 6'-substituted quinoline derivatives bearing methoxy- or bromo-moiety (**1d**, **1i**, respectively). All these 3 compounds reached similar activity as steroidal standard galeterone, but did not outperform the non-steroidal standard enzalutamide, which decreased the AR transcriptional activity below 25%.

Analysing the agonist activities of the studied compounds towards the AR, we have observed that 2 of 8 A-ring-fused quinolines displayed dose dependent agonist activity (**1b** and **1g** in correspondence with the antagonist mode). Two other A-ring fused quinolines exerted moderate agonist activities in 10 μM and 2 μM (**1c**, **1i**), while the rest of this group was found to be no AR agonist, including **1a** and **1d**, which belong to the most potent antagonists and were selected for further experiments.

Despite the fact that there is no generally clear SAR within series **2** and **3**, several characteristics can be pointed out. The monosubstitution at C-6' position of the A-ring fused pyridine by an aromatic moiety clearly led to compounds exerting strong agonist activities in series **2**, except for compounds **2f** and **2g** (bearing a *p*-Cl-phenyl or *p*-Br-phenyl

Table 3
AR transcriptional activity in antagonist and agonist modes.

	cmpd.	AR transcriptional activity **antagonist** mode[a]			AR transcriptional activity **agonist** mode[a]		
		50 μM	10 μM	2 μM	50 μM	10 μM	2 μM
A-ring-fused quinolines	**1a**	4	50	85	3	17	20
	1b	142	121	108	41	30	24
	1c	11	98	104	16	59	43
	1d	16	53	96	5	10	16
	1e	46	96	103	8	14	16
	1f	7	103	114	3	18	19
	1g	110	106	106	93	65	56
	1h	96	67	92	10	10	14
	1i	18	52	102	5	49	53
A-ring-fused 6'-substituted pyridines	**2a**	115	90	94	121	67	66
	2b	196	116	107	190	110	83
	2c	183	136	123	194	133	122
	2d	124	83	93	73	43	30
	2e	151	110	110	146	56	34
	2f	36	85	89	51	69	69
	2g	70	105	105	69	68	53
	2h	116	88	89	19	13	15
A-ring-fused 4',6'-disubstituted pyridines	**3a**	71	105	105	58	43	23
	3b	26	100	102	24	62	34
	3c	4	92	103	5	94	100
	3d	78	100	99	31	23	17
	3e	113	114	111	94	77	57
	3f	99	92	104	85	88	63
	3g	70	111	111	47	40	21
	3h	84	106	113	63	72	64
	3i	113	130	120	89	117	120
	3j	135	129	114	16	16	16
	3k	109	113	110	55	23	16
	3l	167	148	127	143	127	116
	3m	129	111	111	31	19	16
	3n	115	114	112	55	24	16
	3o	163	123	106	120	70	32
	galeterone	8	48	84	3	12	14
	enzalutamide	20	24	46	12	14	14

[a] Transcriptional activity of AR upon 24 h treatment of 22Rv1-ARE14 with analysed compounds in antagonist (competition with standard agonist, 1 nM R1881) and agonist (compound alone) modes, normalised to the signal of 1 nM R1881. Measured in duplicate and repeated twice, mean is presented.

substituent, respectively), which displayed moderate antagonist activity. In series **3**, the combination of a methyl moiety at 4'-position with an aryl substitution in C-6' position of the A-ring fused pyridine yielded compounds with weak to moderate antagonist properties (**3a**–**3c**). Similar beneficial effect was recently observed in very potent disubstituted A-ring fused pyrazoles [17]. In contrast, substitutions by aryl groups in both C-4' and C-6' positions of the pyridine moiety yielded compounds with moderate to strong agonist activities, where the combination of *p*-halophenyl with pyridin-2-yl functionalities at these positions led to the most potent agonists from the series **3**. This observation also correlates with our previous research, where biaryl derivatives of A-ring fused pyrazoles were found to be potent AR agonists [17].

Next, all compounds were evaluated in 20 μM concentration for their effect on PCa cell lines' proliferation using the resazurine-based cell viability assay after 72 h treatment. The collection of PCa cell lines represented LAPC-4 (wild type AR), 22Rv1 (LBD mutation AR-H875Y and splicing variant V-7), LNCaP (LBD mutation T877A) and DU145 (AR negative). It is known that AR antagonists induce only moderate cytotoxicity, since the blockage of AR-mediated signalling leads rather to cytostatic effect. Our results confirmed those studies, because the majority of compounds decreased the viability only to 70–80% of the vehicle-treated cells. Generally, the viability of DU145 was not influenced by most of the compounds, which, in our hypotheses, supports the targeting of the AR (Table 4).

In the 3 most potent antagonists from the A-ring-fused quinoline derivatives (**1a**, **1d**, **1i**), we expected to observe the antiproliferative activity against AR-positive PCa cells. Corresponding with the AR-antagonist activity, compounds **1d** and **1i** indeed displayed reasonable antiproliferative activity predominantly in 22Rv1 (decreasing the viability to approx. 20% of the control treated by vehicle), but also in LAPC-4 and LNCaP. Compound **1d** outperformed the standard antagonist galeterone in 22Rv1 and displayed similar potency to this standard in LNCaP and LAPC-4. There was a clear difference between the sensitivity of the AR-positive cell lines and the AR-negative DU145 (Table 4). Based on the structure of compounds, the unsubstituted A-ring fused quinoline (**1a**) displayed weaker antiproliferative activity compared

Table 4
Viability of PCa cells after 72 h treatment with 20 μM compounds.

	Cmpd.	Viability of Pca cell lines after treatment with 20 μM for 72 h (mean)[a]			
		LNCaP	LAPC-4	22Rv1	DU145
A-ring-fused quinolines	**1a**	80	84	77	98
	1b	85	98	114	88
	1c	83	74	99	104
	1d	56	80	24	89
	1e	92	86	111	103
	1f	80	71	66	92
	1g	84	90	122	106
	1h	94	82	44	97
	1i	81	59	19	84
A-ring-fused 6'-substituted pyridines	**2a**	85	61	91	112
	2b	84	90	113	107
	2c	85	98	75	103
	2d	87	79	82	99
	2e	88	79	106	102
	2f	80	33	67	112
	2g	84	73	73	107
	2h	85	89	87	97
A-ring-fused 4',6'-disubstituted pyridines	**3a**	83	66	124	111
	3b	78	61	98	112
	3c	70	59	49	108
	3d	79	80	69	113
	3e	74	62	70	100
	3f	63	78	70	114
	3g	70	64	56	106
	3h	65	16	67	98
	3i	60	69	81	103
	3j	89	109	86	103
	3k	87	107	84	105
	3l	68	89	96	106
	3m	86	100	85	108
	3n	90	106	89	101
	3o	79	106	113	103
	galeterone	58	76	95	109
	enzalutamide	99	81	102	96

[a] Cytotoxic effect of compounds was evaluated by resazurine-based viability assay (72-hour treatment) with a single dose of 20 μM compounds. Measured in duplicate and repeated twice.

with the 6'- methoxy- or bromo-substituted analogues (**1d**, **1i**, respectively). Interestingly, the most sensitive cell line to these two derivatives was 22Rv1, with less but still notable sensitivity to **1h** (8'-chloroquinoline derivative) and **1f** (6'-chloroquinoline derivative).

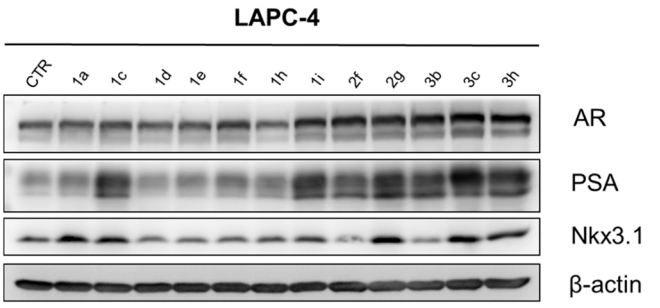

Fig. 6. Several A-ring fused quinolines display agonist mode of action. Effect on AR-signalling was evaluated using immunoblotting in LAPC-4 cells treated with 10 μM concentration of selected compounds for 48 h.

Since the most promising compounds were found within series **1**, we have evaluated the antiproliferative activity of these derivatives in 10 μM towards the LAPC-4 cell line using the colony-formation assay (CFA) for 10 days. Compounds **1a**, **1c**, **1d**, **1g**, **1h** and **1i** decreased the colony-formation to 16–30% of control treated by vehicle, while **1b**, **1e**, and **1f** did not have such effect (Fig. 5).

The perspective members of series **1** (except for **1b** and **1g**) were further tested for their effect on the AR protein level and AR-regulated proteins in LAPC-4 at 10 μM concentration, upon 48-h treatment. We did not observe any profound decreases in AR and AR-regulated proteins. On the other hand, compounds **1c** and **1i** increased the level of PSA. Selected compounds from series **2** (**2f**, **2g**) and **3** (**3b**, **3c** and **3h**) increased the AR and PSA protein level that confirmed their agonist mode of action (Fig. 6). Within analogous experiment in LNCaP, we observed a marked decrease in Nkx3.1 and PSA level upon 48-h treatment with 10 μM of **1d** (Fig. S3). On the other hand, compounds **1a**, **1e**, **1f**, **1h** affected only the Nkx3.1 protein level, by significant decrease in case of **1f** and moderate decrease for the rest (Fig. S3).

Based on all the above-mentioned results, we have evaluated that compound **1d** displayed the highest potency towards the AR transcriptional activity, AR-positive PCa cell lines' viability and beneficial effects on AR signalling, therefore we further evaluated other characteristics of this lead compound.

2.3. Detailed effect of 1d on AR signalling, PCa cells' viability, proliferation, and the cell cycle

We have evaluated the effect of **1d** on the AR-transcriptional activity using the reporter cell line 22Rv1-ARE14 again, in wide concentration range, both in agonist and antagonist modes. It was found that IC_{50} value of **1d** antagonism (10.5 μM) (Fig. 7A) shows weaker, but comparable potency to galeterone (7.6 μM), a known standard antagonist. After

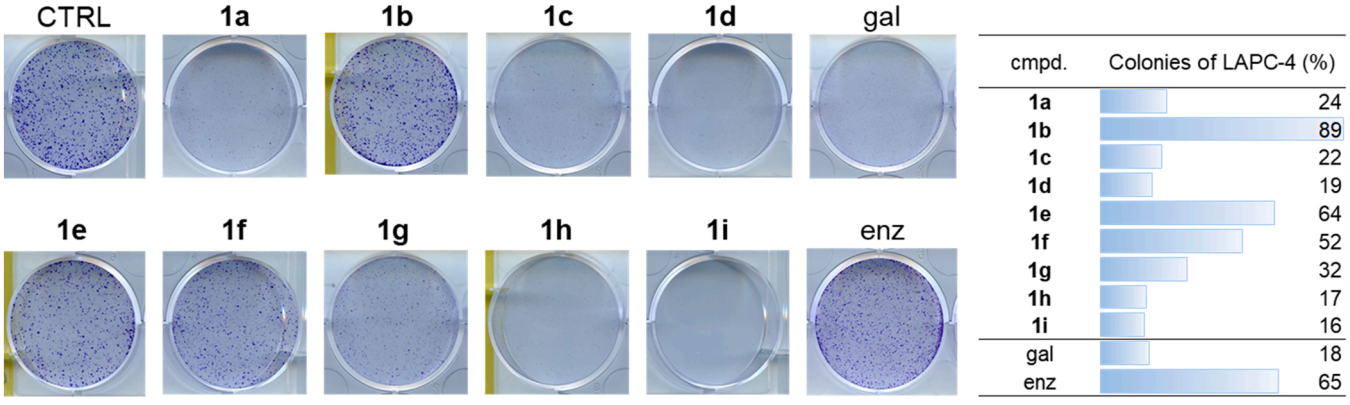

Fig. 5. A-ring fused quinolines reduce LAPC-4 derived colony formation. Antiproliferative activity of compounds from series **1** was evaluated in 10 μM concentration using colony-formation assay (10 days treatment). Gal, galeterone; Enz, enzalutamide.

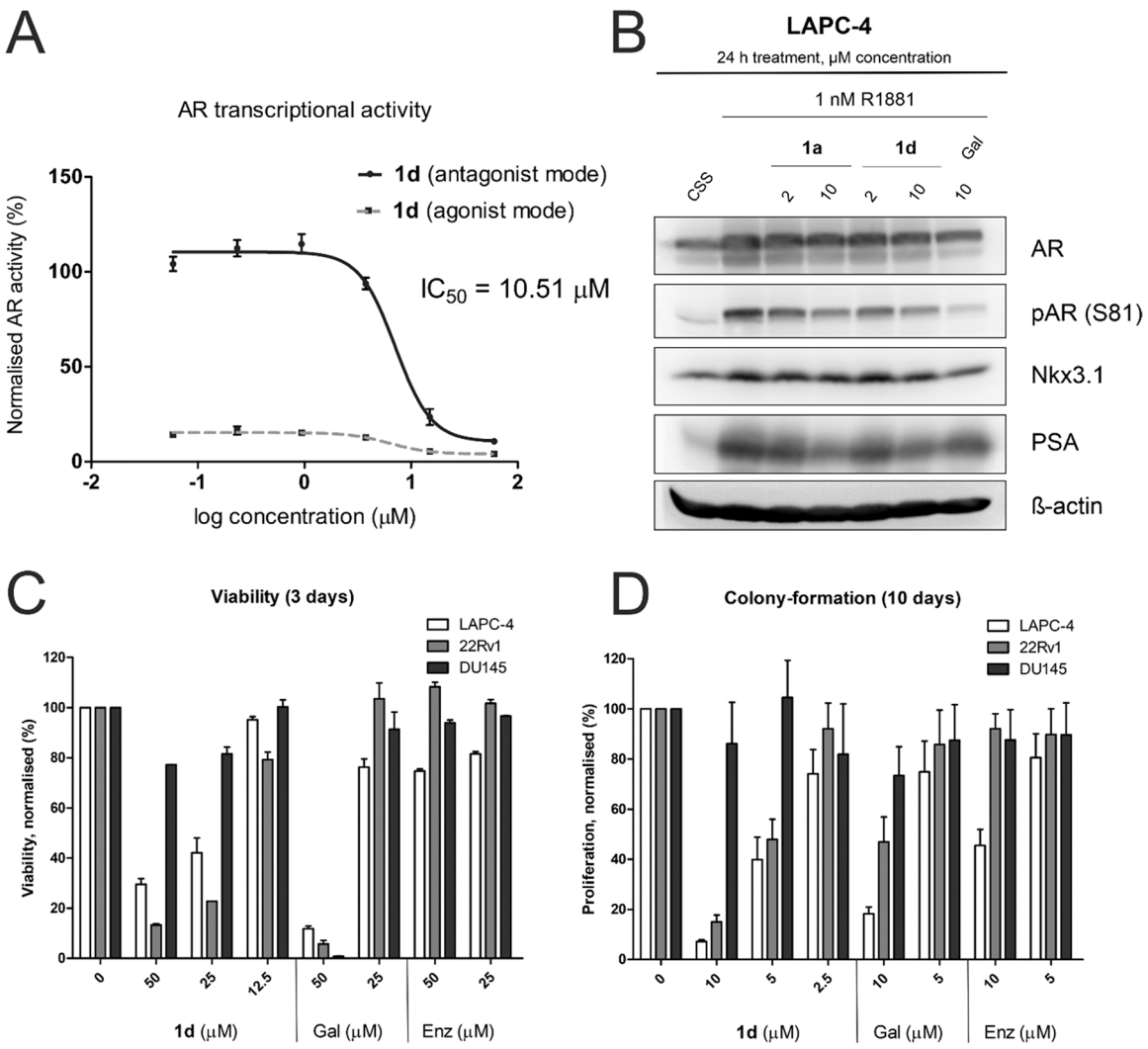

Fig. 7. Compound **1d** acts as a pure antagonist, interferes with AR-downstream signalling and displays selective antiproliferative activity towards AR-positive PCa cell lines. **(A)** Transcriptional activity of AR upon treatment with **1d** in antagonist (competition with standard agonist, 1 nM R1881) and agonist (compound alone) modes, normalised to the signal of 1 nM R1881. Curves were plotted via non-linear curve fit in GraphPad Prism 5 from 4 independent experiments, error bars represent SD. **(B)** Effect of **1a** and **1d** on expression of AR and its downstream targets using immunoblotting. The cells were deprived of androgens (in CSS) for 24 h and stimulated with 1 nM of R1881 alone or with analysed compounds for additional 24 h. **(C)** Cytotoxic effect of **1d** and standards was evaluated by resazurine-based viability assay (3-days treatment), measured in duplicate and repeated twice. **(D)** Antiproliferative activity of **1d** and standards was evaluated using colony-formation assay (10-days treatment) in duplicate and repeated twice. Gal, galeterone; Enz, enzalutamide.

steroid withdrawal and subsequent stimulation of AR signalling by synthetic androgen R1881, we observed the ability of **1d** and **1a** to diminish the AR activating phosphorylation on S81 and suppression of AR signalling in 10 μM concentration (decrease of the PSA protein level), similar to the effect of galeterone (Fig. 7B). We observed similar activity of the lead compound mainly on the PSA level even in LNCaP and 22Rv1 (Fig. S4).

The antiproliferative effect of **1d** was further evaluated in PCa cell lines in dose dependent manner, using both the resazurine-based viability assay upon 3 days of treatment (Fig. 7C) and colony formation assay upon 10 days of treatment (Fig. 7D). We clearly confirmed that **1d** targets preferentially the AR-positive PCa cell lines. Upon 3 days of treatment, compound **1d** was able to decrease the viability of LAPC-4 and 22Rv1 below the 50% of control treated by vehicle at 50 μM and 25 μM, with 22Rv1 being slightly more sensitive. The lead compound outperformed the standard galeterone, which displayed an anti-proliferative activity only at 50 μM after 3 days, and enzalutamide, which exerted moderate antiproliferative effect only in LAPC-4. In contrast with galeterone, which markedly affected also the AR-negative DU145 at 50 μM, we did not observe significant effect of **1d** towards the DU145 cell line (Fig. 7C). In agreement with previous findings, the antiproliferative activity of the lead compound was enhanced after 10 days of treatment, which was assessed by the colony-formation analysis. The lead compound preferentially blocked the formation of LAPC-4 and 22Rv1 cell colonies in dose dependent manner and showed to be more effective than galeterone and enzalutamide (Fig. 7D).

Cell cycle analysis after 24 h of treatment showed an increased number of cells in G1 phase with reduced S-phase cells' percentage, which reflected the proliferation blockage of LAPC-4 and LNCaP, mainly at 10 μM concentration of the lead compound. The effect of **1d** was more profound, in comparison with galeterone or enzalutamide (Fig. S5).

2.4. Interaction of 1d with the AR-LBD and molecular modelling

To verify the ability of **1d** to bind to the AR cavity in cells, we performed "the rescue experiment" in LAPC-4 cells. The cells were treated with **1d** for 2 h to saturate the AR-ligand-binding domain (LBD) and then bavdegalutamide (ARV-110, an effective AR degrader) was added

for additional 6 h. As presented in Fig. 8A, the degradation of AR induced by bavdegalutamide was attenuated by 20 μM of **1d** and confirmed its cellular interaction with the AR cavity.

Next, the interaction of **1d** was also confirmed by the microscale thermophoresis (MST) using His6-tagged human AR-LBD [29]. Binding of **1d** in 12.5 μM and 25 μM concentrations led to an extensive change of the labelling dye-fluorescence (Fig. 8B). Moreover, the change was consistent with the effect of 25 μM galeterone (Fig. 8B).

We recruited the flexible molecular docking of the candidate compound **1d** into AR-LBD co-crystal structure with natural agonist DHT (PDB: 2PIV). The key residues in extremities of the cavity (Asn705, Gln711, Arg752, and Thr877) were set flexible, which allowed rearrangement of the cavity to fit **1d**. The best pose displayed high binding energy ($\Delta G_{Vina} = -10.2$ kcal/mol) and similar orientation as was observed for steroidal antagonists cyproterone [30] or galeterone [31]. Overall, the A-ring fused 6'-methoxyquinoline part was sandwiched between the helix 2 and 3 and the methoxy moiety was oriented towards the Val 684, with possible hydrogen bonds between the oxygen and Arg752 and Gln711. The fused quinoline moiety was stabilised by hydrophobic bonds with Leu707, Met749 and Phe764. Further hydrophobic interactions were formed between the steroid ring and side chains of Leu704, Met780 and Leu873. The 17β-OH on the D-ring formed a conserved bond with Thr877, with a possible interaction with Asn705 as well (Fig. 8C).

3. Conclusions

In conclusion, we reported the efficient syntheses of A-ring-fused mono- and disubstituted pyridine derivatives of DHT in two different synthetic pathways, using microwave irradiation as an energy source. 1,5-Diketones were prepared using Mannich salts, which were then converted to A-ring-fused 6'-substituted pyridines with hydroxylamine. The compound library was extended with 4',6'-disubstituted analogues by the Kröhnke's pyridine synthesis. Single crystal X-ray diffraction confirmed the exact structure of a representative monosubstituted pyridine derivative. Pharmacological investigations were performed in prostate cancer cells in comparison with previously prepared, structurally similar quinolines. It was shown that several A-ring-fused quinolines

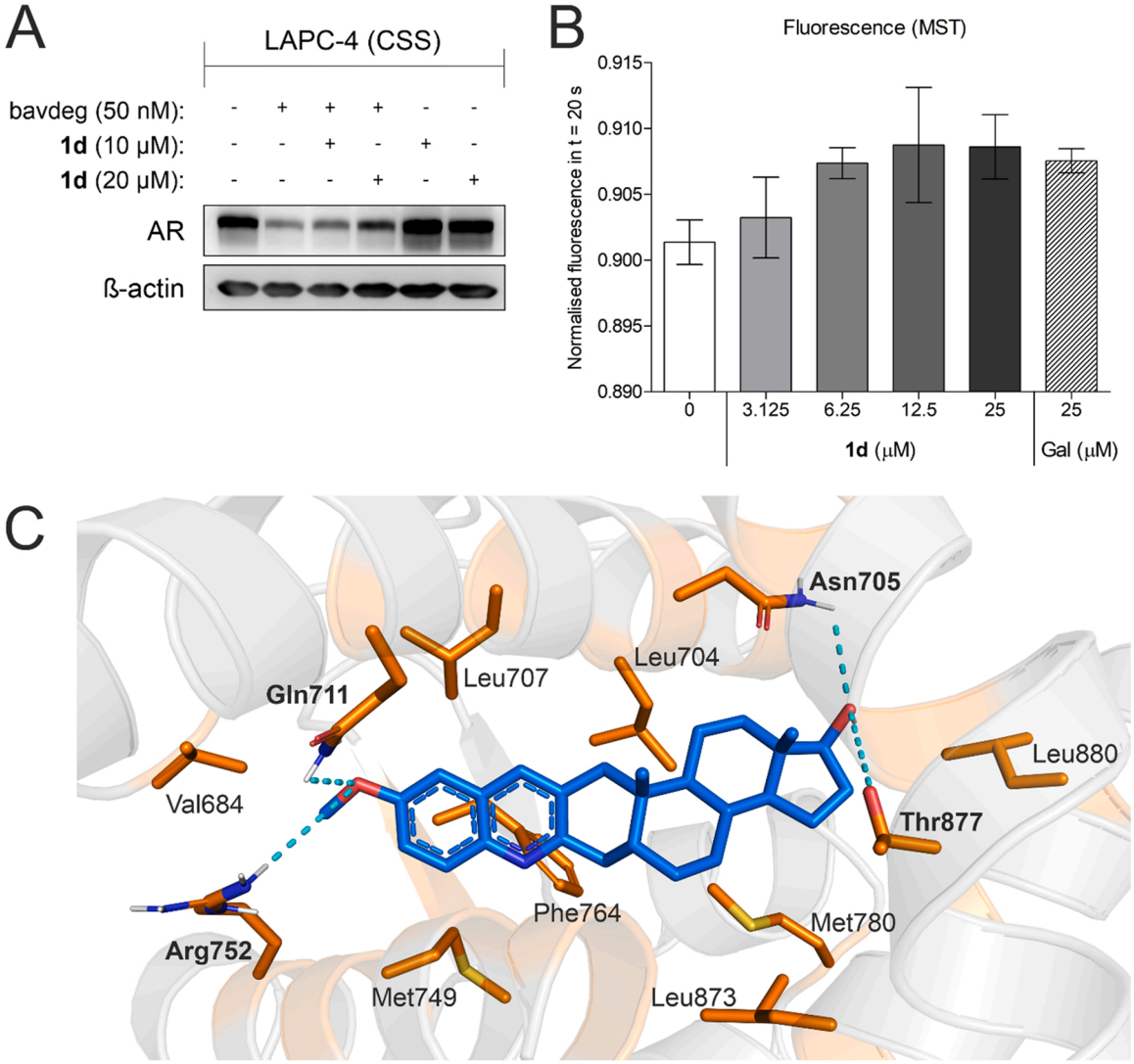

Fig. 8. Compound **1d** binds the AR protein *in vitro* and *in silico*. **(A)** Compound **1d** suppresses bavdegalutamide-induced AR-degradation. LAPC-4 cells were cultivated in CSS-supplemented medium, pre-treated with **1d** for 2 h and then bavdegalutamide was added for the next 6 h. Level of *β*-actin served as protein loading control. Bavdeg, bavdegalutamide. **(B)** Binding of **1d** to recombinant AR was evaluated by MST measurement with His6-tagged human AR-LBD. Bar chart displays the mean ± SD ($n = 2$). Gal, galeterone. **(C)** Binding pose of **1d** in the LBD of AR (PDB: 2PIV) performed by flexible docking. AR protein is shown in grey, orange sticks represent interacting amino acid residues, labelled in bold are residues displaying hydrogen bonds. Nitrogen atoms are shown in blue, oxygen atoms in red, hydrogens in white. Hydrogen bonds are shown as cyan dash lines.

acted as AR antagonists, in comparison with the dual or agonist character of the majority of A-ring-fused pyridines. Based on the antagonist and antiproliferative activity of the whole set of compounds, the best derivative **1d** (6'-methoxy-substituted A-ring fused quinoline) was chosen as the lead compound. It was further studied and showed to be a low-micromolar AR antagonist (IC_{50} = 10.5 μM), it suppressed the viability and proliferation of AR-positive PCa cell lines. Moreover, the candidate compound blocked the AR downstream signalling, induced moderate cell-cycle arrest and was proven to bind the AR in cells and the recombinant AR protein as well. The binding mode and interaction was described using molecular modelling.

4. Experimental

4.1. General

Chemicals, reagents and solvents were purchased from commercial suppliers (Sigma-Aldrich, TCI and Alfa Aesar) and used without further purification. For MW-assisted syntheses, a CEM Discover SP laboratory MW reactor was used with a max. power of 200 W (running a dynamic control program). Elementary analysis data were obtained with a PerkinElmer CHN analyzer model 2400. The transformations were monitored by TLC using 0.25 mm thick Kieselgel-G plates (Si 254 F, Merck). The compound spots were detected by spraying with 5% phosphomolybdic acid in 50% aqueous phosphoric acid. Column chromatography (CC) was carried out on silica gel 60, 40–63 μm (Merck). Melting points (Mp) were determined on an SRS Optimelt digital apparatus and are uncorrected. NMR spectra were recorded with a Bruker DRX 500 instrument at room temperature in $CDCl_3$ using residual solvent signal as an internal reference. Chemical shifts are reported in ppm (δ scale) and coupling constants (J) are given in Hz. Multiplicities of the ^{1}H signals are indicated as a singlet (s), a doublet (d), a double doublet (dd), a triplet (t), or a multiplet (m). ^{13}C NMR spectra are ^{1}H-decoupled and the J-MOD pulse sequence was used for multiplicity editing. In this spin-echo type experiment, the signal intensity is modulated by the different coupling constants J of carbons depending on the number of attached protons. Both protonated and unprotonated carbons can be detected (CH_3 and CH carbons appear as positive signals, while CH_2 and C carbons as negative signals). The purified derivatives were dissolved in high purity acetonitrile and introduced with an Agilent 1290 Infinity II liquid chromatography pump to an Agilent 6470 tandem mass spectrometer equipped an electrospray ionization chamber. Flow rate was 0.5 mL·min− 1 and contained 0.1% formic acid or 0.1% ammonium hydroxide to help facilitate ionization. The instrument operated in MS1 scan mode with 135 V fragmentor voltage, and the spectra were recorded from 300 to 500 m/z, which were corrected with the background.

4.2. Chemistry

4.2.1. General procedure for the synthesis of A-ring-fused 6'-substituted pyridine derivatives of DHT (2a–h)

DHT (290 mg, 1 mmol) and the corresponding Mannich salt (**4a**–**h**, 2 equiv.) were dissolved in 1,4-dioxane (5 mL), and pyrrolidine (246 μL, 3 equiv.) was added. The mixture was irradiated in a closed vessel at 120 °C for 20 min. After completion of the reaction, the mixture was cooled to room temperature, and the solvent was evaporated under reduced pressure. The brown oil thus obtained was dissolved in absolute EtOH (10 mL), then hydroxylamine hydrochloride (83 mg, 1.2 equiv.) was added and the mixture was irradiated in a closed vessel at 90 °C for 10 min. During work-up, the mixture was cooled to room temperature, poured into water (20 mL) and saturated $NaHCO_3$ solution was added to neutralize the reaction mixture. The water phase was extracted with CH_2Cl_2 (2 × 10 mL). The combined organic layer was washed with water (2 × 10 mL) and brine (20 mL), dried over anhydrous Na_2SO_4 and the solvent was evaporated under reduced pressure to yield a brown oil, which was then purified by CC with a pure solvent or solvent mixture as described in each subchapter containing 1 v/v% TEA.

4.2.1.1. 6'-Phenylpyridino[2',3':3,2]-5α-androstan-17β-ole (**2a**). According to Section 4.2.1., **4a** (427 mg) was used. The crude product was purified by CC (CH_2Cl_2). Yield: 326 mg (81%, off white solid). Mp 213–216 °C; ^{1}H NMR ($CDCl_3$, 500 MHz): δ_H 0.77 (s, 3 H, 18-H_3), 0.81 (s, 3 H, 19-H_3), 0.81–1.02 (overlapping m, 3 H, 9α-H, 7α-H and 14α-H), 1.13 (m, 1 H, 12α-H), 1.24–1.52 (overlapping m, 5 H, 15β-H, 11β-H, 6β-H, 8β-H and 16β-H), 1.60–1.70 (overlapping m, 4 H, 11α-H, 5α-H, 15α-H and 6α-H), 1.77 (m, 1 H, 7β-H), 1.88 (m, 1 H, 12β-H), 2.07 (m, 1 H, 16α-H), 2.51 (d, 1 H, J = 16.3 Hz, 1α-H), 2.76–2.83 (overlapping dd and d, 2 H, 4β-H and 1β-H), 3.25 (m, 1 H, 4α-H), 3.66 (m, 1 H, 17α-H), 7.42 (t-like m, 1 H, 4''-H), 7.48 (t-like m, 2 H, 3''-H and 5''-H), 7.52 (d, 1 H, J = 7.9 Hz) and 7.56 (d, 1 H, J = 7.9 Hz): 4'-H and 5'-H, 7,99 (d, 2 H, J = 7.2 Hz, 2''-H and 6''-H); ^{13}C NMR ($CDCl_3$, 125 MHz): δ_C 11.2 (C-18), 11.9 (C-19), 21.1 (C-11), 23.6 (C-15), 28.7 (C-6), 30.8 (C-16), 31.4 (C-7), 35.4 (C-10), 35.9 (C-8), 37.0 (C-4), 37.1 (C-12), 42.4 (C-5), 43.1 (C-13), 43.3 (C-1), 51.2 (C-14), 54.1 (C-9), 82.1 (C-17), 118.1 (C-5'), 127.0 (2 C, C-2'' and C-6''), 128.5 (C-4''), 128.7 (2 C, C-3'' and C-5''), 129.9 (C-2), 138.1 (C-4'), 140.0 (C-1''), 154.9 (C-6'), 156.4 (C-3); ESI-MS 402 $[M+H]^+$; Anal. Calcd. for $C_{28}H_{35}NO$ C 83.74; H 8.78. Found C 83.63; H 8.76.

4.2.1.2. 6'-(*p*-Tolyl)pyridino[2',3':3,2]-5α-androstan-17β-ole (**2b**). According to Section 4.2.1., **4b** (455 mg) was used. The crude product was purified by CC (CH_2Cl_2). Yield: 290 mg (70%, off white solid). Mp 251–254 °C; ^{1}H NMR ($CDCl_3$, 500 MHz): δ_H 0.78 (s, 3 H, 18-H_3), 0.81 (s, 3 H, 19-H_3), 0.83–1.03 (overlapping m, 3 H), 1.12 (m, 1 H), 1.25–1.52 (overlapping m, 5 H), 1.62–1.72 (overlapping m, 4 H), 1.76 (m, 1 H), 1.88 (m, 1 H), 2.07 (m, 1 H, 16α-H), 2.39 (s, 3 H, 4''-CH_3), 2.47 (d, 1 H, J = 16.2 Hz, 1α-H), 2.67 (dd, 1 H, J = 18.0 Hz, J = 12.6 Hz, 4β-H), 2.75 (d, 1 H, J = 16.2 Hz, 1β-H), 2.93 (dd, 1 H, J = 18.0 Hz, J = 5.2 Hz, 4α-H), 3.66 (t, 1 H, J = 8.3 Hz, 17α-H), 7.24 (d, 2 H, J = 7.9 Hz, 3''-H and 5''-H), 7.36 (d, 1 H, J = 7.9 Hz, 4'-H), 7.43 (d, 1 H, J = 7.9 Hz, 5'-H), 7.85 (d, 2 H, J = 7.9 Hz, 2''-H and 6''-H); ^{13}C NMR ($CDCl_3$, 125 MHz): δ_C 11.2 (C-18), 11.9 (C-19), 21.1 (C-11), 21.4 (4''-CH_3), 23.6 (C-15), 28.8 (C-6), 30.8 (C-16), 31.4 (C-7), 35.4 (C-10), 35.9 (C-8), 37.0 (C-4), 37.1 (C-12), 42.4 (C-5), 43.1 (C-13), 43.3 (C-1), 51.2 (C-14), 54.1 (C-9), 82.1 (C-17), 117.8 (C-5'), 126.8 (2 C, C-2'' and C-6''), 129.5 (2 C, C-3'' and C-5''), 129.5 (C-4''), 137.3 (C-2), 138.0 (C-4'), 138.4 (C-1''), 154.9 (C-6'), 156.3 (C-3); ESI-MS 416 $[M+H]^+$; Anal. Calcd. for $C_{29}H_{37}NO$ C 83.81; H 8.97. Found C 83.95; H 8.99.

4.2.1.3. 6'-(*p*-Methoxyphenyl)pyridino[2',3':3,2]-5α-androstan-17β-ole (**2c**). According to Section 4.2.1., **4c** (487 mg) was used. The crude product was purified by CC (CH_2Cl_2). Yield: 342 mg (79%, off white solid). Mp 230–233 °C; ^{1}H NMR ($CDCl_3$, 500 MHz): δ_H 0.78 (s, 3 H, 18-H_3), 0.81 (s, 3 H, 19-H_3), 0.85 (m, 1 H), 0.93–1.02 (overlapping m, 2 H), 1.12 (m, 1 H), 1.24–1.52 (overlapping m, 5 H), 1.60–1.77 (overlapping m, 5 H), 1.87 (m, 1 H), 2.07 (m, 1 H, 16α-H), 2.46 (d, 1 H, J = 16.2 Hz, 1α-H), 2.67 (dd, 1 H, J = 18.0 Hz, J = 12.5 Hz, 4β-H), 2.75 (d, 1 H, J = 16.2 Hz, 1β-H), 2.91 (dd, 1 H, J = 18.0 Hz, J = 5.3 Hz, 4α-H), 3.66 (t, 1 H, J = 8.6 Hz, 17α-H), 3.85 (s, 3 H, 4''-OMe), 6.97 (d, 2 H, J = 8.8 Hz, 3''-H and 5''-H), 7.35 (d, 1 H, J = 8.0 Hz, 4'-H), 7.40 (d, 1 H, J = 8.0 Hz, 5'-H), 7.90 (d, 2 H, J = 8.8 Hz, 2''-H and 6''-H); ^{13}C NMR ($CDCl_3$, 125 MHz): δ_C 11.2 (C-18), 11.9 (C-19), 21.1 (C-11), 23.6 (C-15), 28.7 (C-6), 30.7 (C-16), 31.4 (C-7), 35.4 (C-10), 35.8 (C-8), 36.9 (C-4), 37.1 (C-12), 42.3 (C-5), 43.0 (C-13), 43.2 (C-1), 51.1 (C-14), 54.0 (C-9), 55.5 (4''-OMe), 82.1 (C-17), 114.1 (2 C, C-3'' and C-5''), 117.4 (C-5'), 128.1 (2 C, C-2'' and C-6''), 129.1 (C-1''), 132.7 (C-2), 138.1 (C-4'), 154.5 (C-6'), 156.2 (C-3), 160.2 (C-4''); ESI-MS 432 $[M+H]^+$; Anal. Calcd. for $C_{29}H_{37}NO_2$ C 80.70; H 8.64. Found C 80.88; H 8.67.

4.2.1.4. 6'-(*p*-Nitrophenyl)pyridino[2',3':3,2]-5α-androstan-17β-ole (**2d**). According to Section 4.2.1., **4d** (517 mg) was used. The crude product was purified by CC (EtOAc/CH_2Cl_2 = 2:98). Yield: 321 mg (72%, light yellow solid). Mp > 250 °C decomposes; ^{1}H NMR ($CDCl_3$, 500 MHz): δ_H 0.78 (s, 3 H, 18-H_3), 0.82 (s, 3 H, 19-H_3), 0.88 (m, 1 H), 0.95–1.04 (overlapping m, 2 H), 1.13 (m, 1 H), 1.28–1.53 (overlapping m, 5 H), 1.60–1.72 (overlapping m, 4 H), 1.77 (m, 1 H), 1.88 (m, 1 H),

2.08 (m, 1 H, 16α-H), 2.51 (d, 1 H, $J = 16.4$ Hz, 1α-H), 2.69 (dd, 1 H, $J = 18.2$ Hz, $J = 12.4$ Hz, 4β-H), 2.82 (d, 1 H, $J = 16.4$ Hz, 1β-H), 2.95 (dd, 1 H, $J = 18.2$ Hz, $J = 5.3$ Hz, 4α-H), 3.67 (t, 1 H, $J = 8.3$ Hz, 17α-H), 7.46 (d, 1 H, $J = 8.0$ Hz, 4'-H), 7.54 (d, 1 H, $J = 8.0$ Hz, 5'-H), 8.14 (d, 2 H, $J = 8.7$ Hz, 2''-H and 6''-H), 8.29 (d, 2 H, $J = 8.7$ Hz, 3''-H and 5''-H); ^{13}C NMR ($CDCl_3$, 125 MHz): δ_C 11.2 (C-18), 11.9 (C-19), 21.1 (C-11), 23.6 (C-15), 28.7 (C-6), 30.7 (C-16), 31.3 (C-7), 35.4 (C-10), 35.8 (C-8), 36.9 (C-4), 37.0 (C-12), 42.3 (C-5), 43.0 (C-13), 43.3 (C-1), 51.1 (C-14), 53.9 (C-9), 82.1 (C-17), 118.7 (C-5'), 124.1 (2 C, C-3'' and C-5''), 127.6 (2 C, C-2'' and C-6''), 131.9 (C-2), 138.4 (C-4'), 145.9 (C-1''), 147.9 (C-4''), 152.0 (C-6'), 157.2 (C-3); ESI-MS 447 $[M+H]^+$; Anal. Calcd. for $C_{28}H_{34}N_2O_3$ C 75.31; H 7.67. Found C 75.08; H 7.66.

4.2.1.5. 6'-(*p*-Fluorophenyl)pyridino[2',3':3,2]-5α-androstan-17β-ole (**2e**). According to Section 4.2.1., **4e** (463 mg) was used. The crude product was purified by CC (EtOAc/CH_2Cl_2 = 2:98). Yield: 337 mg (80%, off white solid). Mp > 200 °C decomposes; ^{1}H NMR ($CDCl_3$, 500 MHz): δ_H 0.78 (s, 3 H, 18-H_3), 0.81 (s, 3 H, 19-H_3), 0.87–1.03 (overlapping m, 3 H), 1.13 (m, 1 H), 1.25–1.53 (overlapping m, 5 H), 1.61–1.72 (overlapping m, 4 H), 1.76 (m, 1 H), 1.88 (m, 1 H), 2.07 (m, 1 H, 16α-H), 2.48 (d, 1 H, $J = 16.2$ Hz, 1α-H), 2.67 (dd, 1 H, $J = 18.1$ Hz, $J = 12.6$ Hz, 4β-H), 2.77 (d, 1 H, $J = 16.2$ Hz, 1β-H), 2.92 (dd, 1 H, $J = 18.1$ Hz, $J = 5.2$ Hz, 4α-H), 3.66 (t, 1 H, $J = 8.5$ Hz, 17α-H), 7.11 (t, 2 H, $J = 8.7$ Hz, 3''-H and 5''-H), 7.38 (d, 1 H, $J = 8.0$ Hz, 4'-H), 7.41 (d, 1 H, $J = 8.0$ Hz, 5'-H), 7.94 (dd, 2 H, $J = 8.7$ Hz, $J = 5.5$ Hz, 2''-H and 6''-H); ^{13}C NMR ($CDCl_3$, 125 MHz): δ_C 11.2 (C-18), 11.9 (C-19), 21.1 (C-11), 23.6 (C-15), 28.7 (C-6), 30.8 (C-16), 31.4 (C-7), 35.4 (C-10), 35.9 (C-8), 37.0 (C-4), 37.1 (C-12), 42.4 (C-5), 43.1 (C-13), 43.2 (C-1), 51.2 (C-14), 54.1 (C-9), 82.1 (C-17), 115.6 (2 C, $J = 21.4$ Hz, C-3'' and C-5''), 117.7 (C-5'), 128.7 (2 C, $J = 8.2$ Hz, C-2'' and C-6''), 129.9 (C-2), 136.2 ($J = 2.9$ Hz, C-1''), 138.2 (C-4'), 153.8 (C-6'), 156.5 (C-3), 163.5 ($J = 247.5$ Hz, (C-4''); ESI-MS 420 $[M+H]^+$; Anal. Calcd. for $C_{28}H_{34}FNO$ C 80.15; H 8.17. Found C 79.94; H 8.15.

4.2.1.6. 6'-(*p*-Chlorophenyl)pyridino[2',3':3,2]-5α-androstan-17β-ole (**2f**). According to Section 4.2.1., **4f** (496 mg) was used. The crude product was purified by CC (EtOAc/CH_2Cl_2 = 5:95). Yield: 313 mg (72%, off white solid). Mp > 200 °C decomposes; ^{1}H NMR ($CDCl_3$, 500 MHz): δ_H 0.78 (s, 3 H, 18-H_3), 0.81 (s, 3 H, 19-H_3), 0.86 (m, 1 H), 0.91–1.03 (overlapping m, 2 H), 1.13 (m, 1 H), 1.23–1.52 (overlapping m, 5 H), 1.59–1.72 (overlapping m, 4 H), 1.76 (m, 1 H), 1.87 (m, 1 H), 2.08 (m, 1 H, 16α-H), 2.47 (d, 1 H, $J = 16.3$ Hz, 1α-H), 2.67 (dd, 1 H, $J = 18.0$ Hz, $J = 12.7$ Hz, 4β-H), 2.77 (d, 1 H, $J = 16.3$ Hz, 1β-H), 2.92 (dd, 1 H, $J = 18.0$ Hz, $J = 5.1$ Hz, 4α-H), 3.66 (t, 1 H, $J = 8.3$ Hz, 17α-H), 7.38–7.44 (overlapping m, 4 H, 4'-H, 5'-H, 3''-H and 5''-H), 7.90 (d, 2 H, $J = 8.2$ Hz, 2''-H and 6''-H); ^{13}C NMR ($CDCl_3$, 125 MHz): δ_C 11.2 (C-18), 11.9 (C-19), 21.1 (C-11), 23.6 (C-15), 28.7 (C-6), 30.7 (C-16), 31.4 (C-7), 35.4 (C-10), 35.8 (C-8), 36.9 (C-4), 37.1 (C-12), 42.3 (C-5), 43.0 (C-13), 43.2 (C-1), 51.1 (C-14), 54.0 (C-9), 82.1 (C-17), 117.9 (C-5'), 128.5 (2 C, C-3'' and C-5''), 131.9 (2 C, C-2'' and C-6''), 130.3 (C-2), 134.6 (C-4''), 138.2 (C-4'), 138.4 (C-1''), 153.5 (C-6'), 156.6 (C-3); ESI-MS 436 $[M+H]^+$; Anal. Calcd. for $C_{28}H_{34}ClNO$ C 77.13; H 7.86. Found C 77.23; H 7.88.

4.2.1.7. 6'-(*p*-Bromophenyl)pyridino[2',3':3,2]-5α-androstan-17β-ole (**2g**). According to Section 4.2.1., **4g** (585 mg) was used. The crude product was purified by CC (EtOAc/CH_2Cl_2 = 5:95). Yield: 374 mg (78%, off white solid). Mp 223–226 °C; ^{1}H NMR ($CDCl_3$, 500 MHz): δ_H 0.78 (s, 3 H, 18-H_3), 0.81 (s, 3 H, 19-H_3), 0.86 (m, 1 H), 0.92–1.03 (overlapping m, 2 H), 1.13 (m, 1 H), 1.25–1.53 (overlapping m, 5 H), 1.60–1.72 (overlapping m, 4 H), 1.77 (m, 1 H), 1.88 (m, 1 H), 2.08 (m, 1 H, 16α-H), 2.47 (d, 1 H, $J = 16.3$ Hz, 1α-H), 2.67 (dd, 1 H, $J = 18.1$ Hz, $J = 12.5$ Hz, 4β-H), 2.77 (d, 1 H, $J = 16.3$ Hz, 1β-H), 2.92 (dd, 1 H, $J = 18.1$ Hz, $J = 5.3$ Hz, 4α-H), 3.66 (m, 1 H, 17α-H), 7.38 (d, 1 H, $J = 8.0$ Hz, 4'-H), 7.43 (d, 1 H, $J = 8.0$ Hz, 5'-H), 7.56 (d, 2 H, $J = 8.4$ Hz, 3''-H and 5''-H), 7.84 (d, 2 H, $J = 8.4$ Hz, 2''-H and 6''-H); ^{13}C NMR ($CDCl_3$, 125 MHz): δ_C 11.2 (C-18), 11.9 (C-19), 21.1 (C-11), 23.6 (C-15), 28.7 (C-6), 30.8 (C-16), 31.4 (C-7), 35.4 (C-10), 35.9 (C-8), 37.0 (C-4), 37.1 (C-12), 42.4 (C-5), 43.1 (C-13), 43.3 (C-1), 51.2 (C-14), 54.1 (C-9), 82.1 (C-17), 117.8 (C-5'), 122.9 (C-4''), 128.5 (2 C, C-2'' and C-6''), 130.4 (C-2), 131.9 (2 C, C-3'' and C-5''), 138.2 (C-4'), 138.9 (C-1''), 153.6 (C-6'), 156.6 (C-3); ESI-MS 480 $[M+H]^+$; Anal. Calcd. for $C_{28}H_{34}BrNO$ C 69.99; H 7.13. Found C 70.12; H 7.14.

4.2.1.8. 6'-(*o*-Hydroxyphenyl)pyridino[2',3':3,2]-5α-androstan-17β-ole (**2h**). According to Section 4.2.1., **4h** (459 mg) was used. The crude product was purified by CC (CH_2Cl_2). Yield: 278 mg (67%, white solid). Mp 298–300 °C; ^{1}H NMR ($CDCl_3$, 500 MHz): δ_H 0.78 (s, 3 H, 18-H_3), 0.80 (s, 3 H, 19-H_3), 0.86 (m, 1 H), 0.94–1.02 (overlapping m, 2 H), 1.13 (m, 1 H), 1.26–1.52 (overlapping m, 5 H), 1.60–1.70 (overlapping m, 4 H), 1.76 (m, 1 H), 1.88 (m, 1 H), 2.08 (m, 1 H, 16α-H), 2.47 (d, 1 H, $J = 16.3$ Hz, 1α-H), 2.65 (dd, 1 H, $J = 18.0$ Hz, 12.5 Hz, 4β-H), 2.77 (d, 1 H, $J = 16.3$ Hz, 1β-H), 2.86 (dd, 1 H, $J = 18.0$ Hz, $J = 5.1$ Hz, 4α-H), 3.66 (m, 1 H, 17α-H), 6.88 (t-like m, 1 H, 4''-H), 7.00 (d, 1 H, $J = 8.2$ Hz, 6''-H), 7.26 (t-like m, 1 H, 5''-H), 7.48 (d, 1 H, $J = 8.3$ Hz, 4'-H), 7.66 (d, 1 H, $J = 8.3$ Hz, 5'-H), 7.77 (d, 1 H, $J = 8.0$ Hz, 3''-H), 14.78 (s, 1 H, Ph-OH); ^{13}C NMR ($CDCl_3$, 125 MHz): δ_C 11.2 (C-18), 11.9 (C-19), 21.1 (C-11), 23.6 (C-15), 28.5 (C-6), 30.7 (C-16), 31.3 (C-7), 35.5 (C-10), 35.7 (C-8), 36.0 (C-4), 36.9 (C-12), 42.0 (C-1), 42.9 (C-5), 43.0 (C-13), 51.1 (C-14), 53.9 (C-9), 82.1 (C-17), 116.5 (C-6''), 118.6 and 118.7 (C-5' and C-5''), 119.2 (C-2''), 126.0 (C-4''), 129.7 (C-2), 131.0 (C-3''), 139.2 (C-4'), 153.0 (C-6'), 155.1 (C-1''), 160.3 (C-3); ESI-MS 418 $[M+H]^+$; Anal. Calcd. for $C_{28}H_{35}NO_2$ C 80.53; H 8.45. Found C 80.49; H 8.42.

4.2.2. General procedure for the synthesis of A-ring-fused 4',6'-disubstituted pyridine derivatives of DHT (3a–o)

2-Ethylidene (**5a**) or 2-arylidene (**5b–e**) derivative (1.0 mmol), appropriate pyridinium iodide salt (**6a–c**, 1.4 equiv.) and ammonium acetate (771 mg, 10.0 equiv.) were suspended in absolute EtOH (5 mL), and the mixture was irradiated in a closed vessel at 90 °C for 20 min. After completion of the reaction, the mixture was cooled to room temperature, poured into water (20 mL) and extracted with CH_2Cl_2 (2 × 10 mL). The combined organic layer was washed with water (2 × 10 mL) and brine (20 mL), dried over anhydrous Na_2SO_4 and the solvent was evaporated under reduced pressure. The crude product thus obtained was purified by CC with a pure solvent or solvent mixture as described in each subchapter containing 1 v/v% TEA.

4.2.2.1. 4'-Methyl-6'-phenylpyridino[2',3':3,2]-5α-androstan-17β-ole (**3a**). According to Section 4.2.2., **5a** (316 mg) and **6a** (455 mg) were used. The crude product was purified by CC (EtOAc/hexane = 30:70). Yield: 298 mg (72%, white solid). Mp 263–265 °C; ^{1}H NMR ($CDCl_3$, 500 MHz): δ_H 0.79 (s, 3 H, 18-H_3), 0.82 (s, 3 H, 19-H_3), 0.86–1.04 (overlapping m, 3 H), 1.15 (m, 1 H), 1.25–1.55 (overlapping m, 5 H), 1.61–1.66 (overlapping m, 3 H), 1.75 (overlapping m, 2 H), 1.89 (m, 1 H), 2.08 (m, 1 H, 16α-H), 2.23 (d, 1 H, $J = 16.6$ Hz, 1α-H), 2.27 (s, 3 H, 4'-CH_3), 2.69–2.77 (overlapping dd and d, 2 H, 4β-H and 1β-H), 2.90 (dd, 1 H, $J = 17.9$ Hz, $J = 5.0$ Hz, 4α-H), 3.67 (m, 1 H, 17α-H), 7.36 (overlapping m, 2 H, 5'-H and 4''-H), 7.43 (t, 2 H, $J = 7.6$ Hz, 3''-H and 5''-H), 7.94 (d, 2 H, $J = 7.4$ Hz, 2''-H and 6''-H); ^{13}C NMR ($CDCl_3$, 125 MHz): δ_C 11.2 (C-18), 12.3 (C-19), 19.6 (4'-CH_3), 21.1 (C-11), 23.6 (C-15), 28.6 (C-6), 30.8 (C-16), 31.4 (C-7), 35.2 (C-10), 35.8 (C-8), 36.9 (C-4), 37.2 (C-12), 40.3 (C-1), 41.9 (C-5), 43.0 (C-13), 51.2 (C-14), 54.3 (C-9), 82.1 (C-17), 119.9 (C-5'), 127.0 (2 C, C-2'' and C-6''), 128.4 (C-4''), 128.7 (2 C, C-3'' and C-5''), 128.8 (C-2), 140.1 (C-1''), 146.7 (C-4'), 154.3 (C-6'), 155.8 (C-3); ESI-MS 416 $[M+H]^+$; Anal. Calcd. for $C_{29}H_{37}NO$ C 83.81; H 8.97. Found C 83.99; H 8.99.

4.2.2.2. 6'-(*o*-Hydoxyphenyl)-4'-methylpyridino[2',3':3,2]-5α-androstan-17β-ole (**3b**). According to Section 4.2.2., **5a** (316 mg) and **6b** (478 mg) were used. The crude product was purified by CC (CH_2Cl_2). Yield: 281 mg (65%, off white solid); Mp 265–267 °C; ^{1}H NMR ($CDCl_3$, 500 MHz): δ_H 0.78 (s, 3 H, 18-H_3), 0.80 (s, 3 H, 19-H_3), 0.84–1.02 (overlapping m, 3 H), 1.14 (m, 1 H), 1.26–1.54 (overlapping m, 5 H), 1.57–1.67 (overlapping m, 3 H), 1.74 (overlapping m, 2 H), 1.89 (m, 1 H), 2.08 (m, 1 H, 16α-H), 2.21 (d, 1 H, $J = 16.7$ Hz, 1α-H), 2.30 (s, 3 H, 4'-CH_3), 2.67 (dd, 1 H, $J = 18.2$ Hz, 12.5 Hz, 4β-H), 2.73 (d, 1 H, $J =$

16.7 Hz, 1β-H), 2.81 (dd, 1 H, J = 18.2 Hz, J = 5.1 Hz, 4α-H), 3.67 (m, 1 H, 17α-H), 6.86 (t, 1 H, J = 7.6 Hz, 4''-H), 7.00 (d, 1 H, J = 8.2 Hz, 6''-H), 7.25 (t-like m, 1 H, 5''-H), 7.52 (s, 1 H, 5'-H), 7.77 (d, 1 H, J = 8.0 Hz, 3''-H), 15.0 (s, 1 H, Ph-OH); ^{13}C NMR ($CDCl_3$, 125 MHz): δ_C 11.2 (C-18), 12.3 (C-19), 19.9 (4'-CH_3), 21.1 (C-11), 23.6 (C-15), 28.4 (C-6), 30.7 (C-16), 31.3 (C-7), 35.3 (C-10), 35.7 (C-8), 36.1 (C-4), 36.9 (C-12), 40.1 (C-1), 41.6 (C-5), 43.0 (C-13), 51.1 (C-14), 54.2 (C-9), 82.1 (C-17), 117.9 (C-6''), 118.5 (2 C, C-4'' and C-5'), 119.1 (C-2''), 125.9 (C-5''), 128.7 (C-2), 130.8 (C-3''), 148.2 (C-4'), 152.2 (C-6'), 154.4 (C-1''), 160.3 (C-3); ESI-MS 432 $[M+H]^+$; Anal. Calcd. for $C_{29}H_{37}NO_2$ C 80.70; H 8.64. Found C 80.51; H 8.61.

4.2.2.3. 4'-Methyl-6'-(pyridin-2''-yl)pyridino[2',3':3,2]-5α-androstan-17β-ole (**3c**). According to Section 4.2.2., **5a** (316 mg) and **6c** (457 mg) were used. The crude product was purified by CC (EtOAc/hexane = 40:60). Yield: 294 mg (71%, off white solid). Mp 226–229 °C; ^{1}H NMR ($CDCl_3$, 500 MHz): δ_H 0.78 (s, 3 H, 18-H_3), 0.81 (s, 3 H, 19-H_3), 0.86–1.03 (overlapping m, 3 H), 1.14 (m, 1 H), 1.25–1.55 (overlapping m, 5 H), 1.60–1.67 (overlapping m, 3 H), 1.76 (overlapping m, 2 H), 1.89 (m, 1 H), 2.08 (m, 1 H, 16α-H), 2.24 (d, 1 H, J = 16.7 Hz, 1α-H), 2.29 (s, 3 H, 4'-CH_3), 2.69–2.79 (overlapping dd and d, 2 H, 4β-H and 1β-H), 2.90 (dd, 1 H, J = 17.8 Hz, J = 4.8 Hz, 4α-H), 3.67 (t, 1 H, J = 8.5 Hz, 17α-H), 7.25 (t-like m, 1 H, 5''-H), 7.77 (t, 1 H, J = 7.7 Hz, 4''-H), 7.97 (s, 1 H, 5'-H), 8.35 (d, 1 H, J = 8.0 Hz, 3''-H), 8.65 (d, 1 H, J = 4.9 Hz, 6''-H); ^{13}C NMR ($CDCl_3$, 125 MHz): δ_C 11.2 (C-18), 12.3 (C-19), 19.5 (C-4'), 21.1 (C-11), 23.6 (C-15), 28.6 (C-6), 30.7 (C-16), 31.4 (C-7), 35.2 (C-10), 35.8 (C-8), 36.9 (C-4), 37.2 (C-12), 40.5 (C-1), 41.9 (C-5), 43.0 (C-13), 51.2 (C-14), 54.3 (C-9), 82.1 (C-17), 120.2 (C-5'), 121.1 (C-3''), 123.3 (C-5''), 130.7 (C-2), 136.9 (C-4''), 147.1 (C-4'), 149.2 (C-6''), 152.8 (C-6'), 155.5 and 157.0: C-2'' and C-3; ESI-MS 417 $[M+H]^+$; Anal. Calcd. for $C_{28}H_{36}N_2O$ C 80.73; H 8.71. Found C 80.95; H 8.74.

4.2.2.4. 4',6'-Diphenylpyridino[2',3':3,2]-5α-androstan-17β-ole (**3d**). According to Section 4.2.2., **5b** (379 mg) and **6a** (455 mg) were used. The crude product was purified by CC (EtOAc/hexane = 20:80). Yield: 368 mg (77%, white solid). Mp 139–142 °C; ^{1}H NMR ($CDCl_3$, 500 MHz): δ_H 0.72 (s, 3 H, 18-H_3), 0.75 (s, 3 H, 19-H_3), 0.81 (m, 1 H), 0.91–1.07 (overlapping m, 3 H), 1.23–1.46 (overlapping m, 5 H), 1.59–1.76 (overlapping m, 6 H), 2.06 (m, 1 H, 16α-H), 2.32 (d, 1 H, J = 16.5 Hz, 1α-H), 2.68–2.79 (overlapping dd and d, 2 H, 4β-H and 1β-H), 3.05 (dd, 1 H, J = 18.1 Hz, J = 5.4 Hz, 4α-H), 3.63 (t, 1 H, J = 8.4 Hz, 17α-H), 7.33–7.48 (overlapping m, 9 H, Ph-H^4, Ph-H^3, Ph-H^5, Ph-H^2, Ph-H^6, 4''-H, 3''-H, 5''-H and 5'-H), 7.98 (d, 2 H, J = 7.7 Hz, 2''-H and 6''-H); ^{13}C NMR ($CDCl_3$, 125 MHz): δ_C 11.2 (C-18), 11.8 (C-19), 21.0 (C-11), 23.6 (C-15), 28.6 (C-6), 30.7 (C-16), 31.4 (C-7), 35.5 (C-10), 35.8 (C-8), 36.8 (C-4), 37.6 (C-12), 41.4 (C-1), 42.1 (C-5), 43.0 (C-13), 51.1 (C-14), 54.0 (C-9), 82.1 (C-17), 119.5 (C-5'), 127.0 (2 C, C-2'' and C-6''), 127.4 (C-2), 127.9 (Ph-C^4), 128.5 (2 C, Ph-C^2 and Ph-C^6), 128.6 (C-4''), 128.7 (2 C, Ph-C^3 and Ph-C^5), 128.8 (2 C, C-3'' and C-5''), 139.9 and 140.0: Ph-C^1 and C-1'', 150.9 (C-4'), 154.4 (C-6'), 156.9 (C-3); ESI-MS 478 $[M+H]^+$; Anal. Calcd. for $C_{34}H_{39}NO$ C 85.49; H 8.23. Found C 85.19; H 8.20.

4.2.2.5. 6'-(*o*-Hydoxyphenyl)-4'-phenylpyridino[2',3':3,2]-5α-androstan-17β-ole (**3e**). According to Section 4.2.2., **5b** (379 mg) and **6b** (478 mg) was used. The crude product was purified by CC (EtOAc/CH_2Cl_2 = 2:98). Yield: 377 mg (76%, off white solid). Mp 146–149 °C; ^{1}H NMR ($CDCl_3$, 500 MHz): δ_H 0.71 (s, 3 H, 18-H_3), 0.74 (s, 3 H, 19-H_3), 0.80 (m, 1 H), 0.87–1.06 (overlapping m, 3 H), 1.22–1.46 (overlapping m, 6 H), 1.57–1.76 (overlapping m, 5 H), 2.06 (m, 1 H, 16α-H), 2.30 (d, 1 H, J = 16.5 Hz, 1α-H), 2.66 (d, 1 H, J = 16.5 Hz, 1β-H), 2.71 (dd, 1 H, J = 18.0 Hz, 12.4 Hz, 4β-H), 3.05 (dd, 1 H, J = 18.1 Hz, J = 5.5 Hz, 4α-H), 3.62 (m, 1 H, 17α-H), 6.85 (t, 1 H, J = 7.5 Hz, 4''-H), 7.00 (d, 1 H, J = 8.2 Hz, 6''-H), 7.27 (t-like m, 1 H, 5''-H), 7.32 (d, 2 H, J = 7.1 Hz, Ph-H^2 and Ph-H^6), 7.44 (t-like m, 1 H, Ph-H^4), 7.48 (t-like m, 2 H, Ph-H^3 and Ph-H^5), 7.58 (s, 1 H, 5'-H), 7.76 (d, 1 H, J = 7.9 Hz, 3''-H), 14.82 (s, 1 H, Ph-OH); ^{13}C NMR ($CDCl_3$, 125 MHz): δ_C 11.2 (C-18), 11.8 (C-19), 20.9 (C-11), 23.5 (C-15), 28.5 (C-6), 30.7 (C-16), 31.3 (C-7), 35.5 (C-10), 35.7 (C-8), 36.5 (C-4), 36.8 (C-12), 41.2 (C-1), 41.8 (C-5), 42.9 (C-13), 51.1 (C-14), 53.9 (C-9), 82.1 (C-17), 117.8 (C-6''), 118.6 and 118.7 (C-4'' and C-5'), 119.1 (C-2''), 126.1 (C-5''), 127.3 (C-2), 128.3 (Ph-C^4), 128.6 (2 C, Ph-C^2 and Ph-C^6), 128.7 (2 C, Ph-C^3 and Ph-C^5), 131.1 (C-3''), 139.4 (Ph-C^1), 152.2 (C-4'), 153.4 (C-6'), 154.6 (C-1''), 160.3 (C-3); ESI-MS 494 $[M+H]^+$; Anal. Calcd. for $C_{34}H_{39}NO_2$ C 82.72; H 7.96. Found C 82.98; H 7.97.

4.2.2.6. 4'-Phenyl-6'-(pyridin-2''-yl)pyridino[2',3':3,2]-5α-androstan-17β-ole (**3f**). According to Section 4.2.2., **5b** (379 mg) and **6c** (457 mg) were used. The crude product was purified by CC (EtOAc/hexane = 40:60). Yield: 391 mg (82%, white solid). Mp 156–159 °C; ^{1}H NMR ($CDCl_3$, 500 MHz): δ_H 0.72 (s, 3 H, 18-H_3), 0.75 (s, 3 H, 19-H_3), 0.81 (m, 1 H), 0.91–1.06 (overlapping m, 3 H), 1.22–1.46 (overlapping m, 5 H), 1.60–1.76 (overlapping m, 6 H), 2.06 (m, 1 H, 16α-H), 2.34 (d, 1 H, J = 16.7 Hz, 1α-H), 2.72–2.80 (overlapping dd and d, 2 H, 4β-H and 1β-H), 3.05 (dd, 1 H, J = 18.1 Hz, J = 5.5 Hz, 4α-H), 3.62 (t-like m, 1 H, 17α-H), 7.26 (t-like m, 1 H, 5''-H), 7.35 (d, 2 H, J = 7.7 Hz, Ph-H^2 and Ph-H^6), 7.39 (t-like m, 1 H, Ph-H^4), 7.44 (t-like m, 2 H, Ph-H^3 and Ph-H^5), 7.79 (t, 1 H, J = 7.7 Hz, 4''-H), 8.04 (s, 1 H, 5'-H), 8.39 (d, 1 H, J = 8.0 Hz, 3''-H), 8.64 (d, 1 H, J = 4.3 Hz, 6''-H); ^{13}C NMR ($CDCl_3$, 125 MHz): δ_C 11.2 (C-18), 11.8 (C-19), 21.0 (C-11), 23.6 (C-15), 28.7 (C-6), 30.7 (C-16), 31.4 (C-7), 35.5 (C-10), 35.8 (C-8), 36.8 (C-4), 37.6 (C-12), 41.6 (C-1), 42.1 (C-5), 43.0 (C-13), 51.2 (C-14), 54.0 (C-9), 82.1 (C-17), 119.9 (C-5'), 121.2 (C-3''), 123.4 (C-5''), 127.8 (Ph-C^4), 128.4 (2 C, Ph-C^2 and Ph-C^6), 128.8 (2 C, Ph-C^3 and Ph-C^5), 129.1 (C-2), 136.9 (C-4''), 139.8 (Ph-C^1), 149.3 (C-6''), 151.2 (C-4'), 153.1 (C-6'), 156.5 and 156.8: C-2'' and C-3; ESI-MS 479 $[M+H]^+$; Anal. Calcd. for $C_{33}H_{38}N_2O$ C 82.80; H 8.00. Found C 82.58; H 7.98.

4.2.2.7. 4'-(*p*-Fluorophenyl)-6'-penylpyridino[2',3':3,2]-5α-androstan-17β-ole (**3g**). According to Section 4.2.2., **5c** (397 mg) and **6a** (455 mg) were used. The crude product was purified by CC (EtOAc/hexane = 20:80). Yield: 334 mg (67%, white solid). Mp 209–211 °C; ^{1}H NMR ($CDCl_3$, 500 MHz): δ_H 0.72 (s, 3 H, 18-H_3), 0.75 (s, 3 H, 19-H_3), 0.81 (m, 1 H), 0.92–1.08 (overlapping m, 3 H), 1.23–1.47 (overlapping m, 6 H), 1.59–1.78 (overlapping m, 5 H), 2.06 (m, 1 H, 16α-H), 2.30 (d, 1 H, J = 16.5 Hz, 1α-H), 2.65 (d, 1 H, J = 16.5 Hz, 1β-H), 2.75 (dd, 1 H, J = 18.0 Hz, J = 12.5 Hz, 4β-H), 3.05 (dd, 1 H, J = 18.1 Hz, J = 5.3 Hz, 4α-H), 3.64 (m, 1 H, 17α-H), 7.16 (t, 2 H, J = 8.4 Hz, Ph-H^3 and Ph-H^5), 7.30 (t-like m, 2 H, Ph-H^2 and Ph-H^6), 7.38 (overlapping m, 2 H, 4''-H and 5'-H), 7.45 (t, 2 H, J = 7.4 Hz, 3''-H and 5''-H), 7.97 (d, 2 H, J = 7.7 Hz, 2''-H and 6''-H); ^{13}C NMR ($CDCl_3$, 125 MHz): δ_C 11.2 (C-18), 11.8 (C-19), 21.0 (C-11), 23.6 (C-15), 28.6 (C-6), 30.7 (C-16), 31.4 (C-7), 35.5 (C-10), 35.8 (C-8), 36.8 (C-4), 37.6 (C-12), 41.4 (C-1), 42.1 (C-5), 43.0 (C-13), 51.1 (C-14), 54.0 (C-9), 82.1 (C-17), 115.6 (d, J = 21.3, Ph-C^3 and Ph-C^5), 119.4 (C-5'), 127.0 (2 C, C-2'' and C-6''), 127.4 (C-2), 128.7 (C-4''), 128.8 (2 C, C-3'' and C-5''), 130.5 (d, 2 C, J = 8.1 Hz, Ph-C^2 and Ph-C^6), 135.9 (d, J = 3.4 Hz, Ph-C^1), 139.7 (C-1''), 149.9 (C-4'), 154.5 (C-6'), 157.0 (C-3), 162.6 (d, J = 247.2 Hz, Ph-C^4); ESI-MS 496 $[M+H]^+$; Anal. Calcd. for $C_{34}H_{38}FNO$ C 82.39; H 7.73. Found C 82.57; H 7.75.

4.2.2.8. 4'-(*p*-Fluorophenyl)-6'-(*o*-hydoxyphenyl)-pyridino[2',3':3,2]-5α-androstan-17β-ole (**3h**). According to Section 4.2.2., **5c** (397 mg) and **6b** (478 mg) were used. The crude product was purified by CC (EtOAc/CH_2Cl_2 = 2:98). Yield: 301 mg (59%; off white solid). Mp > 110 °C decomposes; ^{1}H NMR ($CDCl_3$, 500 MHz): δ_H 0.72 (s, 3 H, 18-H_3), 0.73 (s, 3 H, 19-H_3), 0.81 (m, 1 H), 0.87–1.08 (overlapping m, 3 H), 1.23–1.47 (overlapping m, 6 H), 1.57–1.79 (overlapping m, 5 H), 2.07 (m, 1 H, 16α-H), 2.29 (d, 1 H, J = 16.6 Hz, 1α-H), 2.63 (d, 1 H, J = 16.5 Hz, 1β-H), 2.71 (dd, 1 H, J = 18.1 Hz, 12.3 Hz, 4β-H), 2.96 (dd, 1 H, J = 18.2 Hz, J = 5.2 Hz, 4α-H), 3.63 (t, 1 H, J = 8.3 Hz, 17α-H), 6.86 (t, 1 H, J = 7.5 Hz, 4''-H), 7.01 (d, 1 H, J = 8.2 Hz, 6''-H), 7.18 (t, 2 H, J = 7.9 Hz, Ph-H^3 and Ph-H^5), 7.29 (overlapping m, 3 H, 5''-H, Ph-H^2 and Ph-H^6), 7.56 (s, 1 H, 5'-H), 7.76 (d, 1 H, J = 7.9 Hz, 3''-H), 14.73 (s, 1 H, Ph-OH); ^{13}C NMR ($CDCl_3$, 125 MHz): δ_C 11.2 (C-18), 11.8 (C-19), 21.0 (C-11), 23.5 (C-15), 28.5 (C-6), 30.7 (C-16), 31.3 (C-7), 35.6 (C-10),

35.7 (C-8), 36.5 (C-4), 36.8 (C-12), 41.3 (C-1), 41.8 (C-5), 43.0 (C-13), 51.1 (C-14), 53.9 (C-9), 82.1 (C-17), 115.8 (d, J = 21.4, Ph-C^3 and Ph-C^5), 117.8 (C-6''), 118.6 and 118.7 (C-4'' and C-5'), 118.9 (C-2''), 126.1 (C-5''), 127.3 (C-2), 130.4 (d, 2 C, J = 8.1 Hz, Ph-C^2 and Ph-C^6), 131.2 (C-3''), 135.3 (d, J = 3.4 Hz, Ph-C^1), 151.2 (C-4'), 153.6 (C-6'), 154.7 (C-1''), 160.3 (C-3), 162.7 (d, J = 247.8 Hz, Ph-C^4); ESI-MS 512 $[M+H]^+$; Anal. Calcd. for $C_{34}H_{38}FNO_2$ C 79.81; H 7.49. Found C 79.57; H 7.47.

4.2.2.9. 4'-(*p*-Fluorophenyl)-6'-(pyridin-2''-yl)pyridino[2',3':3,2]-5α-androstan-17β-ole (**3i**). According to Section *4.2.2.*, **5c** (397 mg) and **6c** (457 mg) were used. The crude product was purified by CC (EtOAc/hexane = 40:60). Yield: 339 mg (68%, off white solid). Mp 148–151 °C; ^{1}H NMR ($CDCl_3$, 500 MHz): δ_H 0.72 (s, 3 H, 18-H_3), 0.74 (s, 3 H, 19-H_3), 0.81 (m, 1 H), 0.92–1.07 (overlapping m, 3 H), 1.22–1.46 (overlapping m, 6 H), 1.58–1.78 (overlapping m, 5 H), 2.06 (m, 1 H, 16α-H), 2.32 (d, 1 H, J = 16.6 Hz, 1α-H), 2.69 (d, 1 H, J = 16.6 Hz, 1β-H), 2.75 (dd, 1 H, J = 18.0 Hz, 12.5 Hz, 4β-H), 3.05 (dd, 1 H, J = 18.2 Hz, J = 5.2 Hz, 4α-H), 3.63 (t, 1 H, J = 8.5 Hz, 17α-H), 7.13 (t, 2 H, J = 8.5 Hz, Ph-H^3 and Ph-H^5), 7.27 (m, 1 H, 5''-H), 7.32 (t-like m, 2 H, Ph-H^2 and Ph-H^6), 7.79 (t, 1 H, J = 7.7 Hz, 4''-H), 8.03 (s, 1 H, 5'-H), 8.40 (d, 1 H, J = 8.0 Hz, 3''-H), 8.64 (d, 1 H, J = 4.5 Hz, 6''-H); ^{13}C NMR ($CDCl_3$, 125 MHz): δ_C 11.2 (C-18), 11.8 (C-19), 21.0 (C-11), 23.6 (C-15), 28.6 (C-6), 30.7 (C-16), 31.3 (C-7), 35.5 (C-10), 35.8 (C-8), 36.8 (C-4), 37.5 (C-12), 41.6 (C-1), 42.1 (C-5), 43.0 (C-13), 51.1 (C-14), 54.0 (C-9), 82.1 (C-17), 115.5 (d, J = 21.4, Ph-C^3 and Ph-C^5), 119.8 (C-5'), 121.2 (C-3''), 123.5 (C-5''), 129.2 (C-2), 130.5 (d, 2 C, J = 7.9 Hz, Ph-C^2 and Ph-C^6), 135.7 (d, J = 3.3 Hz, Ph-C^1), 137.0 (C-4''), 149.3 (C-6''), 150.2 (C-4'), 153.1 (C-6'), 156.6 and 156.7: C-2'' and C-3, 162.6 (d, J = 246.9 Hz, Ph-C^4); ESI-MS 497 $[M+H]^+$; Anal. Calcd. for $C_{33}H_{37}FN_2O$ C 79.80; H 7.51. Found C 79.91; H 7.52.

4.2.2.10. 4'-(*p*-Chlorophenyl)-6'-penylpyridino[2',3':3,2]-5α-androstan-17β-ole (**3j**). According to Section *4.2.2.*, **5d** (413 mg) and **6a** (455 mg) were used. The crude product was purified by CC (EtOAc/hexane = 20:80). Yield: 374 mg (73%, white solid). Mp 164–167 °C; ^{1}H NMR ($CDCl_3$, 500 MHz): δ_H 0.72 (s, 3 H, 18-H_3), 0.74 (s, 3 H, 19-H_3), 0.81 (m, 1 H), 0.91–1.08 (overlapping m, 3 H), 1.23–1.47 (overlapping m, 6 H), 1.59–1.79 (overlapping m, 5 H), 2.06 (m, 1 H, 16α-H), 2.30 (d, 1 H, J = 16.5 Hz, 1α-H), 2.65 (d, 1 H, J = 16.5 Hz, 1β-H), 2.75 (dd, 1 H, J = 18.1 Hz, J = 12.5 Hz, 4β-H), 3.05 (dd, 1 H, J = 18.2 Hz, J = 5.3 Hz, 4α-H), 3.64 (t-like m, 1 H, 17α-H), 7.27 (m, 2 H, Ph-H^3 and Ph-H^5), 7.38 (overlapping m, 2 H, 5'-H and 4''-H), 7.44 (overlapping m, 4 H, Ph-H^2, Ph-H^6, 3''-H and 5''-H), 7.97 (d, 2 H, J = 7.9 Hz, 2''-H and 6''-H); ^{13}C NMR ($CDCl_3$, 125 MHz): δ_C 11.2 (C-18), 11.8 (C-19), 21.0 (C-11), 23.6 (C-15), 28.6 (C-6), 30.7 (C-16), 31.3 (C-7), 35.5 (C-10), 35.8 (C-8), 36.8 (C-4), 37.6 (C-12), 41.4 (C-1), 42.1 (C-5), 43.0 (C-13), 51.1 (C-14), 54.0 (C-9), 82.1 (C-17), 119.3 (C-5'), 127.0 (2 C, C-2'' and C-6''), 127.2 (C-2), 128.7 (C-4''), 128.8 (4 C, C-3'', C-5'', Ph-C^3 and Ph-C^5), 130.1 (2 C, Ph-C^2 and Ph-C^6), 134.0 (Ph-C^4), 138.3 (Ph-C^1), 139.7 (C-1''), 149.7 (C-4'), 154.5 (C-6'), 157.1 (C-3); ESI-MS 512 $[M+H]^+$; Anal. Calcd. for $C_{34}H_{38}ClNO$ C 79.74; H 7.48. Found C 79.56; H 7.45.

4.2.2.11. 4'-(*p*-Chlorophenyl)-6'-(*o*-hydoxyphenyl)-pyridino[2',3':3,2]-5α-androstan-17β-ole (**3k**). According to Section *4.2.2.*, **5d** (413 mg) and **6b** (478 mg) were used. The crude product was purified by CC (EtOAc/CH_2Cl_2 = 2:98). Yield: 379 mg (70%, light yellow solid). Mp 260–263 °C; ^{1}H NMR ($CDCl_3$, 500 MHz): δ_H 0.73 (s, 3 H, 18-H_3), 0.74 (s, 3 H, 19-H_3), 0.81 (m, 1 H), 0.91–1.00 (overlapping m, 2 H), 1.06 (m, 1 H), 1.23–1.47 (overlapping m, 6 H), 1.59–1.79 (overlapping m, 5 H), 2.07 (m, 1 H, 16α-H), 2.29 (d, 1 H, J = 16.6 Hz, 1α-H), 2.62 (d, 1 H, J = 16.6 Hz, 1β-H), 2.71 (dd, 1 H, J = 18.1 Hz, 12.5 Hz, 4β-H), 2.97 (dd, 1 H, J = 18.2 Hz, J = 5.3 Hz, 4α-H), 3.64 (t-like m, 1 H, 17α-H), 6.86 (t, 1 H, J = 7.5 Hz, 4''-H), 7.01 (d, 1 H, J = 8.2 Hz, 6''-H), 7.27 (overlapping m, 3 H, 5''-H, Ph-H^3 and Ph-H^5), 7.47 (d, 2 H, J = 7.7 Hz, Ph-H^2 and Ph-H^6), 7.55 (s, 1 H, 5'-H), 7.75 (d, 1 H, J = 8.0 Hz, 3''-H), 14.69 (s, 1 H, Ph-OH); ^{13}C NMR ($CDCl_3$, 125 MHz): δ_C 11.2 (C-18), 11.8 (C-19), 21.0 (C-11), 23.5 (C-15), 28.5 (C-6), 30.7 (C-16), 31.3 (C-7), 35.6 (C-10), 35.7 (C-8), 36.5 (C-4), 36.8 (C-12), 41.2 (C-1), 41.8 (C-5), 43.0 (C-13), 51.1 (C-14), 53.9 (C-9), 82.1 (C-17), 117.6 (C-6''), 118.6 and 118.7 (C-4'' and C-5'), 118.9 (C-2''), 126.1 (C-5''), 127.2 (C-2), 129.0 (2 C, Ph-C^3 and Ph-C^5), 130.0 (2 C, Ph-C^2 and Ph-C^6), 131.2 (C-3''), 134.5 (Ph-C^4), 137.8 (Ph-C^1), 150.9 (C-4'), 153.7 (C-6'), 154.8 (C-1''), 160.3 (C-3); ESI-MS 528 $[M+H]^+$; Anal. Calcd. for $C_{34}H_{38}ClNO_2$ C 77.32; H 7.25. Found C 77.08; H 7.22.

4.2.2.12. 4'-(*p*-Chlorophenyl)-6'-(pyridin-2''-yl)pyridino[2',3':3,2]-5α-androstan-17β-ole (**3l**). According to Section *4.2.2.*, **5d** (413 mg) and **6c** (457 mg) were used. The crude product was purified by CC (EtOAc/hexane = 40:60). Yield: 394 mg (77%, off white solid). Mp 142–145 °C; ^{1}H NMR ($CDCl_3$, 500 MHz): δ_H 0.72 (s, 3 H, 18-H_3), 0.74 (s, 3 H, 19-H_3), 0.81 (m, 1 H), 0.93–1.07 (overlapping m, 3 H), 1.22–1.46 (overlapping m, 6 H), 1.59–1.78 (overlapping m, 5 H), 2.05 (m, 1 H, 16α-H), 2.32 (d, 1 H, J = 16.6 Hz, 1α-H), 2.68 (d, 1 H, J = 16.6 Hz, 1β-H), 2.75 (dd, 1 H, J = 18.0 Hz, 12.5 Hz, 4β-H), 3.05 (dd, 1 H, J = 18.1 Hz, J = 5.3 Hz, 4α-H), 3.63 (t, 1 H, J = 8.5 Hz, 17α-H), 7.27 (m, 1 H, 5''-H),7.29 (d, 2 H, J = 7.9 Hz, Ph-H^3 and Ph-H^5), 7.42 (d, 2 H, J = 7.9 Hz, Ph-H^2 and Ph-H^6), 7.79 (t, 1 H, J = 7.7 Hz, 4''-H), 8.02 (s, 1 H, 5'-H), 8.40 (d, 1 H, J = 8.0 Hz, 3''-H), 8.64 (d, 1 H, J = 4.6 Hz, 6''-H); ^{13}C NMR ($CDCl_3$, 125 MHz): δ_C 11.2 (C-18), 11.8 (C-19), 21.0 (C-11), 23.6 (C-15), 28.6 (C-6), 30.7 (C-16), 31.3 (C-7), 35.5 (C-10), 35.8 (C-8), 36.8 (C-4), 37.5 (C-12), 41.6 (C-1), 42.1 (C-5), 43.0 (C-13), 51.1 (C-14), 54.0 (C-9), 82.1 (C-17), 119.7 (C-5'), 121.2 (C-3''), 123.5 (C-5''), 128.7 (2 C, Ph-C^3 and Ph-C^5), 129.0 (C-2), 130.2 (2 C, Ph-C^2 and Ph-C^6), 133.9 (Ph-C^4), 137.0 (C-4''), 138.2 (Ph-C^1), 149.3 (C-6''), 150.0 (C-4'), 153.2 (C-6'), 156.5 and 156.7: C-2'' and C-3; ESI-MS 513 $[M+H]^+$; Anal. Calcd. for $C_{33}H_{37}ClN_2O$ C 77.25; H 7.27. Found C 76.98; H 7.24.

4.2.2.13. 4'-(*p*-Bromophenyl)-6'-penylpyridino[2',3':3,2]-5α-androstan-17β-ole (**3m**). According to Section *4.2.2.*, **5e** (457 mg) and **6a** (455 mg) were used. The crude product was purified by CC (EtOAc/hexane = 20:80). Yield: 292 (52%, white solid). Mp 163–166 °C; ^{1}H NMR ($CDCl_3$, 500 MHz): δ_H 0.73 (s, 3 H, 18-H_3), 0.74 (s, 3 H, 19-H_3), 0.81 (m, 1 H), 0.91–1.08 (overlapping m, 3 H), 1.23–1.47 (overlapping m, 6 H), 1.60–1.79 (overlapping m, 5 H), 2.06 (m, 1 H, 16α-H), 2.30 (d, 1 H, J = 16.5 Hz, 1α-H), 2.65 (d, 1 H, J = 16.5 Hz, 1β-H), 2.75 (dd, 1 H, J = 18.0 Hz, J = 12.5 Hz, 4β-H), 3.05 (dd, 1 H, J = 18.2 Hz, J = 5.2 Hz, 4α-H), 3.64 (m, 1 H, 17α-H), 7.21 (d, 2 H, J = 7.8 Hz, Ph-H^2 and Ph-H^6), 7.38 (overlapping m, 2 H, 5'-H and 4''-H), 7.44 (t, 2 H, J = 7.4 Hz, 3''-H and 5''-H), 7.60 (d, 2 H, J = 7.8 Hz, Ph-H^3 and Ph-H^5), 7.97 (d, 2 H, J = 7.6 Hz, 2''-H and 6''-H); ^{13}C NMR ($CDCl_3$, 125 MHz): δ_C 11.2 (C-18), 11.8 (C-19), 21.0 (C-11), 23.6 (C-15), 28.6 (C-6), 30.7 (C-16), 31.3 (C-7), 35.5 (C-10), 35.8 (C-8), 36.8 (C-4), 37.6 (C-12), 41.4 (C-1), 42.1 (C-5), 43.0 (C-13), 51.1 (C-14), 54.0 (C-9), 82.1 (C-17), 119.2 (C-5'), 122.2 (Ph-C^4), 127.0 (2 C, C-2'' and C-6''), 127.2 (C-2), 128.7 (C-4''), 128.8 (2 C, C-3'' and C-5''), 130.4 (2 C, Ph-C^2 and Ph-C^6), 131.8 (2 C, Ph-C^3 and Ph-C^5), 138.8 (Ph-C^1), 139.6 (C-1''), 149.7 (C-4'), 154.6 (C-6'), 157.1 (C-3); ESI-MS 558 $[M+H]^+$; Anal. Calcd. for $C_{34}H_{38}BrNO$ C 73.37; H 6.88. Found C 73.51; H 6.90.

4.2.2.14. 4'-(*p*-Bromophenyl)-6'-(*o*-hydoxyphenyl)-pyridino[2',3':3,2]-5α-androstan-17β-ole (**3n**). According to Section *4.2.2.*, **5e** (457 mg) and **6b** (478 mg) were used. The crude product was purified by CC (EtOAc/CH_2Cl_2 = 2:98). Yield: 293 mg (51%, light yellow solid). Mp 269–271 °C; ^{1}H NMR ($CDCl_3$, 500 MHz): δ_H 0.73 (s, 3 H, 18-H_3), 0.73 (s, 3 H, 19-H_3), 0.80 (m, 1 H), 0.91–1.00 (overlapping m, 2 H), 1.05 (m, 1 H), 1.23–1.47 (overlapping m, 6 H), 1.59–1.80 (overlapping m, 5 H), 2.07 (m, 1 H, 16α-H), 2.28 (d, 1 H, J = 16.6 Hz, 1α-H), 2.62 (d, 1 H, J = 16.6 Hz, 1β-H), 2.71 (dd, 1 H, J = 18.2 Hz, 12.3 Hz, 4β-H), 2.96 (dd, 1 H, J = 18.2 Hz, J = 5.3 Hz, 4α-H), 3.64 (m, 1 H, 17α-H), 6.86 (t, 1 H, J = 7.5 Hz, 4''-H), 7.00 (d, 1 H, J = 8.2 Hz, 6''-H), 7.21 (d, 2 H, J = 7.8 Hz, Ph-H^2 and Ph-H^6), 7.27 (t-like m, 1 H, 5''-H), 7.54 (s, 1 H, 5'-H), 7.62 (d, 2 H, J = 7.8 Hz, Ph-H^3 and Ph-H^5), 7.74 (d, 1 H, J = 8.0 Hz, 3''-H), 14.68 (s, 1 H, Ph-OH); ^{13}C NMR ($CDCl_3$, 125 MHz): δ_C 11.2 (C-18), 11.8 (C-19), 21.0 (C-11), 23.5 (C-15), 28.5 (C-6), 30.7 (C-16), 31.3 (C-7), 35.6 (C-10), 35.7 (C-8), 36.5 (C-4), 36.8 (C-12), 41.2 (C-1), 41.7 (C-

5), 43.0 (C-13), 51.1 (C-14), 53.9 (C-9), 82.1 (C-17), 117.5 (C-6''), 118.6 and 118.8 (C-4'' and C-5'), 118.9 (C-2''), 122.6 (Ph-C^4), 126.0 (C-5''), 127.1 (C-2), 130.3 (2 C, Ph-C^2 and Ph-C^6), 131.2 (C-3''), 131.9 (2 C, Ph-C^3 and Ph-C^5), 138.3 (Ph-C^1), 150.9 (C-4'), 153.7 (C-6'), 154.8 (C-1''), 160.3 (C-3); ESI-MS 574 $[M+H]^+$; Anal. Calcd. for $C_{34}H_{38}BrNO_2$ C 71.32; H 6.69. Found C 71.06; H 6.67.

4.2.2.15. 4'-(*p*-Bromophenyl)-6'-(pyridin-2''-yl)pyridino[2',3':3,2]-5α-androstan-17β-ole (**3o**). According to Section 4.2.2., **5e** (457 mg) and **6c** (457 mg) were used. The crude product was purified by CC (EtOAc/hexane = 40:60). Yield: 303 mg (54%, off white solid). Mp 146–148 °C; ^{1}H NMR ($CDCl_3$, 500 MHz): δ_H 0.73 (s, 3 H, 18-H_3), 0.74 (s, 3 H, 19-H_3), 0.81 (m, 1 H), 0.91–1.00 (overlapping m, 2 H), 1.05 (m, 1 H), 1.23–1.47 (overlapping m, 6 H), 1.59–1.79 (overlapping m, 5 H), 2.06 (m, 1 H, 16α-H), 2.32 (d, 1 H, J = 16.6 Hz, 1α-H), 2.69 (d, 1 H, J = 16.6 Hz, 1β-H), 2.75 (dd, 1 H, J = 18.0 Hz, 12.4 Hz, 4β-H), 3.05 (dd, 1 H, J = 18.1 Hz, J = 5.3 Hz, 4α-H), 3.64 (t, 1 H, J = 8.4 Hz, 17α-H), 7.23 (d, 2 H, J = 7.8 Hz, Ph-H^2 and Ph-H^6), 7.27 (m, 1 H, 5''-H), 7.58 (d, 2 H, J = 7.8 Hz, Ph-H^3 and Ph-H^5), 7.79 (t, 1 H, J = 7.7 Hz, 4''-H), 8.02 (s, 1 H, 5'-H), 8.39 (d, 1 H, J = 8.0 Hz, 3''-H), 8.64 (d, 1 H, J = 4.6 Hz, 6''-H); ^{13}C NMR ($CDCl_3$, 125 MHz): δ_C 11.2 (C-18), 11.8 (C-19), 21.0 (C-11), 23.6 (C-15), 28.6 (C-6), 30.7 (C-16), 31.3 (C-7), 35.5 (C-10), 35.8 (C-8), 36.8 (C-4), 37.5 (C-12), 41.6 (C-1), 42.1 (C-5), 43.0 (C-13), 51.1 (C-14), 54.0 (C-9), 82.1 (C-17), 119.6 (C-5'), 121.1 (C-3''), 122.1 (Ph-C^4), 123.5 (C-5''), 128.9 (C-2), 130.5 (2 C, Ph-C^2 and Ph-C^6), 131.6 (2 C, Ph-C^3 and Ph-C^5), 137.0 (C-4''), 138.7 (Ph-C^1), 149.3 (C-6''), 149.9 (C-4'), 153.2 (C-6'), 156.6 and 156.8: C-2'' and C-3; ESI-MS 559 $[M+H]^+$; Anal. Calcd. for $C_{33}H_{37}BrN_2O$ C 71.09; H 6.69. Found C 71.38; H 6.72.

4.3. X-ray data collection, structure solution and refinement for compound 2a

A colourless prism of **2a** was mounted on a loop and measured by single crystal X-ray diffraction. Intensity data were collected on a Rigaku R-Axis Rapid diffractometer (graphite monochromator; Mo-Kα radiation, λ = 0.71073 Å) at 103(2) K. A numerical absorption correction was applied to the data using NUMABS [32] and CrystalClear [33] software. The structure was solved by direct methods by SIR [34] software and was refined using SHELX [35] program package under WinGX [36] software. The structure was visualized using Mercury [37] software. Selected bond lengths and angles were calculated by PLATON [38] software. The ratio of anomalous scattering centres is low in **2a** and the absolute structure could not be determined on the basis of the diffraction data. The absolute structure parameter is 0.6(16). The handedness of the crystal structure was set on the basis of the known absolute configuration of the molecule. (Friedel coverage: 0.936, Friedel fraction max.: 0.994, Friedel fraction full: 0.998). The weighting scheme applied was $w = 1/[\sigma^2(F_o^2) + (0.04460.4073\,P)^2 + 0.4073\,P]$ where $P = (F_o^2 + 2F_c^2)/3$. Hydrogen atomic positions were calculated from assumed geometries. Hydrogen atoms were included in structure factor calculations, but they were not refined. The isotropic displacement parameters of the hydrogen atoms were approximated from the U(eq) value of the atom they were bonded to. Crystal data and details of the structure determination and refinement are listed in Table 5. Bond lengths and angles respectively are listed in Tables S2 and S3. The crystallographic data file for compound **2a** has been deposited with the Cambridge Crystallographic Database as CCDC 2247232.

Table 5
Crystal data and details of structure refinement.

Empirical formula	C28 H35 N O
Formula weight	401.57
Temperature	103(2)
Radiation and wavelength	Mo-Kα, λ = 0.71073 Å
Crystal system	monoclinic
Space group	*P* 21
Unit cell dimensions	*a* = 9.6396(4)Å *b* = 17.8123(6)Å *c* = 13.1637(5)Å α = 90° β = 93.553(7)° γ = 90°
Volume	2255.91(15)Å^3
Z	4
Density (calculated)	1.182 Mg/m^3
Absorption coefficient, μ	0.070 mm^{-1}
F(000)	872
Crystal colour	colourless
Crystal description	prism
Crystal size	0.65 × 0.57 × 0.47 mm
Absorption correction	numerical
Max. and min. transmission	0.9920.995
θ – range for data collection	3.101 ≤ θ ≤ 27.471°
Index ranges	-12 ≤ *h* ≤ 12;– 23 ≤ *k* ≤ 23;– 17 ≤ *l* ≤ 17
Reflections collected	66,337
Completeness to 2θ	0.998
Absolute structure parameter	0.6(16)
Friedel coverage	0.936
Friedel fraction max.	0.994
Friedel fraction full	0.998
Independent reflections	10,343 [*R*(int) = 0.0698]
Reflections *I*> 2σ(*I*)	8680
Refinement method	full-matrix least-squares on *F*2
Data / restraints / parameters	10,286 /1 /548
Goodness-of-fit on *F*2	1.062
Final *R* indices [*I*> 2σ(*I*)]	*R*1 = 0.0567, *wR*2 = 0.1013
R indices (all data)	*R*1 = 0.0715, *wR*2 = 0.1059
Max. and mean shift/esd	0.000;0.000
Largest diff. peak and hole	0.304;– 0.190 e.Å^{-3}

4.4. Cell lines

The 22Rv1-ARE14 reporter cell line [28] (kind gift from prof. Zdeněk Dvořák from Palacky University Olomouc, Czech Republic), the LNCaP and DU145 cells (purchased from ECACC) were grown in RPMI-1640 medium. The LAPC-4 (kind gift from doc. Jan Bouchal, Palacký University Olomouc and University Hospital Olomouc, Czech Republic) cell line was grown in DMEM medium. All media were supplemented with 10% fetal bovine serum or charcoal-stripped serum (steroid-depleted), 100 IU/mL penicillin, 100 μg/mL streptomycin, 4 mM glutamine and 1 mM sodium pyruvate. Cells were cultivated in a humidified incubator, in 5% CO_2 atmosphere, at 37 °C.

4.5. AR transcriptional luciferase assay

AR-transcriptional luciferase assay was performed using the 22Rv1-ARE14 cells based on the published protocol [17]. The Nunc™ MicroWell™ 96-well optical flat-bottom plate (Thermo Fisher Scientific) were used for luciferase assay and the luminescence of the samples was measured using a Tecan M200 Pro microplate reader (Biotek).

4.6. Cell viability assay

Cells were seeded into the 96-well tissue culture plates. The following day, solutions of compounds were added for 72 h. Upon treatment, the resazurin solution (Sigma Aldrich) was added for 4 h, and then the fluorescence of resorufin was measured at 544 nm/590 nm (excitation/emission) using a Fluoroskan Ascent microplate reader (Labsystems). Percentual viability or GI_{50} value were calculated using GraphPad Prism 5.

4.7. Colony formation assay

Cells were seeded in low density into 6-well plates. After two days, the medium was replaced with fresh medium containing different concentrations of the compounds. Cells were cultivated for 10 days. Then, the medium was discarded, and colonies were fixed with 70% ethanol for 15 min, washed with PBS and stained with crystal violet (1% solution

in 96% ethanol). Finally, wells were washed with PBS and photograph was captured. After drying, cell colonies were dissolved in 1% SDS, collected from the plate and the absorbance of the crystal violet was measured in 570 nm.

4.8. Immunoblotting

Cell pellets were obtained after treatments, washed with PBS and kept frozen at - 80 °C. Lysis of the cell material was performed in ice-cold RIPA (radioimmunoprecipitation assay) buffer supplemented with protease and phosphatase inhibitors. After the ultrasound sonication (10 s with 30% amplitude), supernatants were obtained by centrifugation at 14.000 *g* for 30 min. Protein concentration in supernatants was measured and balanced, proteins were denatured in SDS-loading buffer with heating at 95 °C. After the separation by SDS-PAGE, proteins were electroblotted onto nitrocellulose membranes. For immunodetection, membranes were blocked in 4% BSA and 0.1% Tween 20 in TBS solution and incubated overnight with primary antibodies, subsequently washed and incubated with secondary antibodies conjugated with peroxidase. Peroxidase activity was detected by SuperSignal West Pico reagents (Thermo Scientific) using a CCD camera LAS-4000 (Fujifilm). Primary antibodies were purchased from Santa Cruz Biotechnology (anti-β-actin, clone C4). Primary antibodies were purchased from Merck (anti-α-tubulin, clone DM1A; anti-phosphorylated AR (S81)). Specific antibodies were purchased from Cell Signaling Technology (anti-AR, clone D6F11; anti-PSA/KLK3, clone D6B1; anti-Nkx3.1, clone D2Y1A); anti-rabbit secondary antibody (porcine anti-rabit immunoglobulin serum); anti-mouse secondary antibody (rabbit anti-mouse IgG, clone D3V2A)). All antibodies were diluted in 4% BSA and 0.1% Tween 20 in TBS.

4.9. Cell-cycle analysis

Cells were treated with test compounds for 24 h, they were harvested by trypsinisation, washed with PBS and fixed with 70% ethanol. After rehydration, cells were permeabilised by 2 M HCl, 0.5% Triton X-100. Following neutralization and wash with PBS, the cells were stained with propidium iodide and analyzed by flow cytometry with a 488 nm laser (BD FACS Verse with BD FACSuite software, version 1.0.6.). Cell cycle distribution was analyzed using ModFit LT (Verity Software House, version 5.0).

4.10. Molecular docking

The flexible molecular docking was recruited to model the binding of the candidate compound **1d** into AR-LBD co-crystal structure with natural agonist DHT (PDB: 2PIV). The key residues in extremities of the cavity (Asn705, Gln711, Arg752, and Thr877) were set flexible. The 3D-structures of compound **1d** was obtained and its energy was minimized by molecular mechanics with Avogadro 1.90.0. Polar hydrogens were added to ligands and proteins using the AutoDock Tools program [39] and docking studies were performed using AutoDock Vina 1.05 [40]. Interactions of the candidate compound with the protein and the figure were generated in Pymol ver. 2.0.4 (Schrödinger, LLC).

4.11. Preparation and micro-scale thermophoresis (MST) of AR-LBD

AR-LBD (with His_6-tag) was expressed using recombinant plasmid pET-15b-hAR-663–919, which was a generous gift from Elizabeth Wilson (Addgene plasmid # 89083) in expression bacteria BL21(DE3) pLysS similar to the original protocol [29]. Cells were homogenized in lysis buffer (50 mM Tris, 300 mM KCl, pH 8.0, 5 mM dithiotreitol (DTT), 1 mM mono-thioglycerol (MTG) supplemented with protease inhibitors and 1% Nonidet P-40), using an ultrasound sonicator. Supernatant was clarified by centrifugation at 19,000 *g* for 30 min at 4 °C. The purification was performed using the NGC chromatographic system (Bio-Rad) on Ni^{2+}- metal affinity-Sepharose column (His-Trap, Cytiva), equilibrated with 50 mM Tris, 300 mM KCl, pH 8.0, 5 mM DTT, 1 mM MTG and 50 mM imidazole. After loading, the column was washed with the equilibration buffer, followed by a wash with 100 mM imidazole in the equilibration buffer. Elution was performed by 500 mM imidazole in storage buffer (50 mM Tris, 300 mM KCl, pH 8.0, 5 mM DTT, 1 mM MTG). The imidazole was washed out and the protein was concentrated in the storage buffer up to 0.5 mg/mL using centrifugal filter unit with 10 kDa cutoff (Merck). MST method was used to prove interaction of **1d** with the AR-LBD, which was labelled with the Red-Tris-NTA 2nd generation labelling dye (NanoTemper Technologies) (100 nM dye + 800 nM His-tagged protein) for 30 min on ice. The labelled protein underwent the MST measurements with or without **1d** in final concentration of 400 nM His-tagged protein in the storage buffer, supplemented with 0.1% Tween. Measurements were done on a Monolith NT.115 instrument (NanoTemper Technologies) at 37 °C. Obtained results were evaluated and normalised fluorescence in t = 20 s was used to create a bar chart in GraphPad Prism 5.

Funding

The publication was funded by the University of Szeged Open Access Fund (FundRef, Grant No. 6143).

CRediT authorship contribution statement

Éva Frank, Radek Jorda: Conceptualization, Methodology, Resources, Supervision, Writing – review & editing. **Márton A. Kiss, Ádám Baji**: Chemical synthesis and optimization experiments. **Miroslav Peřina, Jakub Bělíček**: Pharmacological studies. **Laura Bereczki**: Single crystal X-ray analysis. **Miroslav Peřina**: Flexible docking. **Márton A. Kiss**: Structural analysis. **Ádám Baji, Miroslav Peřina, Jakub Bělíček**: Formal analysis and interpretation of data. **Miroslav Peřina, Laura Bereczki, Márton A. Kiss**: Writing – original draft preparation. All authors have read and agreed to the published version of the manuscript.

Declaration of Competing Interest

The authors declare that they have no known competing financial interests or personal relationships that could have appeared to influence the work reported in this paper.

Data availability

Data will be made available on request.

Acknowledgement

The authors gratefully acknowledge financial support from the Palacký University Olomouc (IGA_PrF_2023_012).

Appendix A. Supporting information

Supplementary data associated with this article can be found in the online version at doi:10.1016/j.jsbmb.2023.106315.

References

[1] D. Li, W. Zhou, J. Pang, Q. Tang, B. Zhong, C. Shen, L. Xiao, T. Hou, A magic drug target: Androgen receptor, Med Res Rev. 39 (2019) 1485–1514, https://doi.org/10.1002/med.21558.

[2] A. Paschalis, J.S. de Bono, Prostate Cancer 2020: "The Times They Are a′Changing,", Cancer Cell. 38 (2020) 25–27, https://doi.org/10.1016/j.ccell.2020.06.008.

[3] T. Uo, S.R. Plymate, C.C. Sprenger, The potential of AR-V7 as a therapeutic target, Expert Opin. Ther. Targets 22 (2018) 201–216, https://doi.org/10.1080/14728222.2018.1439016.

[4] S. Saranyutanon, S.K. Srivastava, S. Pai, S. Singh, A.P. Singh, Therapies targeted to androgen receptor signaling axis in prostate cancer: progress, challenges, and hope, Cancers (Basel) 12 (2019) 51, https://doi.org/10.3390/cancers12010051.
[5] X. Jia, X. Han, Targeting androgen receptor degradation with PROTACs from bench to bedside, Biomed. Pharmacother. 158 (2023), 114112, https://doi.org/10.1016/j.biopha.2022.114112.
[6] S. De, A. Kumar S K, S.K. Shah, S. Kazi, N. Sarkar, S. Banerjee, S. Dey, Pyridine: the scaffolds with significant clinical diversity, RSC Adv. 12 (2022) 15385–15406, https://doi.org/10.1039/D2RA01571D.
[7] D. Wang, L. Désaubry, G. Li, M. Huang, S. Zheng, Recent Advances in the Synthesis of C2–Functionalized Pyridines and Quinolines Using *N* -Oxide Chemistry, Adv. Synth. Catal. 363 (2021) 2–39, https://doi.org/10.1002/adsc.202000910.
[8] A. Dorababu, Quinoline: a promising scaffold in recent antiprotozoal drug discovery, ChemistrySelect 6 (2021) 2164–2177, https://doi.org/10.1002/slct.202100115.
[9] O.O. Ajani, K.T. Iyaye, O.T. Ademosun, Recent advances in chemistry and therapeutic potential of functionalized quinoline motifs – a review, RSC Adv. 12 (2022) 18594–18614, https://doi.org/10.1039/D2RA02896D.
[10] T.S. Vasaitis, R.D. Bruno, V.C.O. Njar, CYP17 inhibitors for prostate cancer therapy, J. Steroid Biochem Mol. Biol. 125 (2011) 23–31, https://doi.org/10.1016/J.JSBMB.2010.11.005.
[11] J. Richards, A.C. Lim, C.W. Hay, A.E. Taylor, A. Wingate, K. Nowakowska, C. Pezaro, S. Carreira, J. Goodall, W. Arlt, I.J. McEwan, J.S. de Bono, G. Attard, Interactions of Abiraterone, Eplerenone, and Prednisolone with Wild-type and Mutant Androgen Receptor: A Rationale for Increasing Abiraterone Exposure or Combining with MDV3100, Cancer Res 72 (2012) 2176–2182, https://doi.org/10.1158/0008-5472.CAN-11-3980.
[12] Y.K. Shi, B. Wang, X.L. Shi, Y. di Zhao, B. Yu, H.M. Liu, Synthesis and biological evaluation of new steroidal pyridines as potential anti-prostate cancer agents, Eur. J. Med Chem. 145 (2018) 11–22, https://doi.org/10.1016/J.EJMECH.2017.12.094.
[13] Y.T. Yang, S. Du, S. Wang, X. Jia, X. Wang, X. Zhang, Synthesis of new steroidal quinolines with antitumor properties, Steroids 151 (2019), 108465, https://doi.org/10.1016/J.STEROIDS.2019.108465.
[14] A.I. Ilovaisky, A.M. Scherbakov, V.M. Merkulova, E.I. Chernoburova, M. A. Shchetinina, O.E. Andreeva, D.I. Salnikova, I. v Zavarzin, A.O. Terent'ev, Secosteroid–quinoline hybrids as new anticancer agents, J. Steroid Biochem Mol. Biol. 228 (2023), 106245, https://doi.org/10.1016/J.JSBMB.2022.106245.
[15] M.G. Barthakur, M. Borthakur, R.C. Boruah, Convenient preparation of A-ring fused pyridines from steroidal enamides, Steroids 73 (2008) 1137–1142, https://doi.org/10.1016/J.STEROIDS.2008.04.016.
[16] M.A. Kiss, M. Peřina, V. Bazgier, N. v May, Á. Baji, R. Jorda, É. Frank, Synthesis of dihydrotestosterone derivatives modified in the A-ring with (hetero)arylidene, pyrazolo[1,5-a]pyrimidine and triazolo[1,5-a]pyrimidine moieties and their targeting of the androgen receptor in prostate cancer, J. Steroid Biochem Mol. Biol. 211 (2021), 105904, https://doi.org/10.1016/J.JSBMB.2021.105904.
[17] M. Peřina, M.A. Kiss, G. Mótyán, E. Szczyrbová, M. Eliáš, V. Študent, D. Kurfürstová, M. Kovalová, L. Mada, J. Bouchal, É. Frank, R. Jorda, A-ring-fused pyrazoles of dihydrotestosterone targeting prostate cancer cells via the downregulation of the androgen receptor, Eur. J. Med Chem. 249 (2023), 115086, https://doi.org/10.1016/J.EJMECH.2023.115086.
[18] M. Radaeva, H. Li, E. LeBlanc, K. Dalal, F. Ban, F. Ciesielski, B. Chow, H. Morin, S. Awrey, K. Singh, P.S. Rennie, N. Lallous, A. Cherkasov, Structure-Based Study to Overcome Cross-Reactivity of Novel Androgen Receptor Inhibitors, Cells 11 (2022) 2785, https://doi.org/10.3390/cells11182785.
[19] Á. Baji, A. Gyovai, J. Wölfling, R. Minorics, I. Ocsovszki, I. Zupkó, É. Frank, Microwave-assisted one-pot synthesis of steroid–quinoline hybrids and an evaluation of their antiproliferative activities on gynecological cancer cell lines, RSC Adv. 6 (2016) 27501–27516, https://doi.org/10.1039/C6RA03910C.
[20] H.S.P. Rao, E. Poonguzhali, S.P. Senthilkumar, Microwave-Mediated Facile Synthesis of Steroid-like 1,5–Diketones from Mannich Salts, Synth. Commun. 38 (2008) 937–942, https://doi.org/10.1080/00397910701845514.
[21] D. Sielemann, R. Keuper, N. Risch, Efficient preparation of substituted 5,6,7,8-tetrahydroquinolines and octahydroacridine derivatives, J. Für Prakt. Chem. 341 (1999) 487–491, https://doi.org/10.1002/(SICI)1521-3897(199907)341:5<487::AID-PRAC487>3.0.CO;2-J.
[22] T. Miyakoshi, H. Konno, Improved synthesis of 2,4,6-trialkylpyridines from 1,5-diketoalkanes: the total synthesis of Anibamine, Org. Biomol. Chem. 17 (2019) 2896–2905, https://doi.org/10.1039/C8OB02723D.
[23] G. Roman, M. Mareş, V. Năstasă, A. Novel Antifungal, Agent with Broad Spectrum: 1-(4-Biphenylyl)-3-(1 *H* -imidazol-1-yl)-1-propanone, Arch. Pharm. (Weinh.) 346 (2013) 110–118, https://doi.org/10.1002/ardp.201200287.
[24] S.H. Yoon, E. Lee, D.Y. Cho, H.M. Ko, H.Y. Baek, D.K. Choi, E. Kim, J.Y. Park, Synthesis of 4-(3-oxo-3-phenylpropyl)morpholin-4-ium chloride analogues and their inhibitory activities of nitric oxide production in lipopolysaccharide-induced BV2 cells, Bioorg. Med Chem. Lett. 36 (2021), 127780, https://doi.org/10.1016/J.BMCL.2021.127780.
[25] G. Mótyán, M.K. Gopisetty, R.E. Kiss-Faludy, Á. Kulmány, I. Zupkó, É. Frank, M. Kiricsi, Anti-cancer activity of novel dihydrotestosterone-derived ring A-condensed pyrazoles on androgen non-responsive prostate cancer cell lines, Int J. Mol. Sci. 20 (2019) 2170, https://doi.org/10.3390/ijms20092170.
[26] P. Thapa, R. Karki, M. Yun, T.M. Kadayat, E. Lee, H.B. Kwon, Y. Na, W.J. Cho, N. D. Kim, B.S. Jeong, Y. Kwon, E.S. Lee, Design, synthesis, and antitumor evaluation of 2,4,6-triaryl pyridines containing chlorophenyl and phenolic moiety, Eur. J. Med Chem. 52 (2012) 123–136, https://doi.org/10.1016/J.EJMECH.2012.03.010.
[27] G. Bist, S. Park, C. Song, T.B. Thapa Magar, A. Shrestha, Y. Kwon, E.S. Lee, Dihydroxylated 2,6-diphenyl-4-chlorophenylpyridines: Topoisomerase I and IIα dual inhibitors with DNA non-intercalative catalytic activity, Eur. J. Med Chem. 133 (2017) 69–84, https://doi.org/10.1016/J.EJMECH.2017.03.048.
[28] I. Bartonkova, A. Novotna, Z. Dvorak, Novel Stably Transfected Human Reporter Cell Line AIZ-AR as a Tool for an Assessment of Human Androgen Receptor Transcriptional Activity, PLoS One 10 (2015), e0121316, https://doi.org/10.1371/journal.pone.0121316.
[29] E.B. Askew, R.T. Gampe, T.B. Stanley, J.L. Faggart, E.M. Wilson, Modulation of androgen receptor activation function 2 by testosterone and dihydrotestosterone, J. Biol. Chem. 282 (2007) 25801–25816, https://doi.org/10.1074/JBC.M703268200.
[30] C.E. Bohl, Z. Wu, D.D. Miller, C.E. Bell, J.T. Dalton, Crystal Structure of the T877A Human Androgen Receptor Ligand-binding Domain Complexed to Cyproterone Acetate Provides Insight for Ligand-induced Conformational Changes and Structure-based Drug Design, J. Biol. Chem. 282 (2007) 13648–13655, https://doi.org/10.1074/JBC.M611711200.
[31] V.C.O. Njar, A.M.H. Brodie, Discovery and Development of Galeterone (TOK-001 or VN/124-1) for the Treatment of All Stages of Prostate Cancer, J. Med Chem. 58 (2015) 2077–2087, https://doi.org/10.1021/jm501239f.
[32] N.U.M.A.B.S.: Higashi, T, 1998, rev. 2002. (Rigaku/MSC Inc.).
[33] CrystalClear: SM 1.4.0 (Rigaku/MSC Inc., 2008), (n.d.).
[34] M.C. Burla, R. Caliandro, M. Camalli, B. Carrozzini, G.L. Cascarano, L. de Caro, C. Giacovazzo, G. Polidori, R. Spagna, *SIR2004*: an improved tool for crystal structure determination and refinement, J. Appl. Crystallogr 38 (2005) 381–388, https://doi.org/10.1107/S002188980403225X.
[35] S.H.E.L.X.L.: Sheldrick, G.M, 2013, SHELXL-2013 Program for Crystal Structure Solution, University of Göttingen, Germany.
[36] L.J. Farrugia, *WinGX* suite for small-molecule single-crystal crystallography, J. Appl. Crystallogr 32 (1999) 837–838, https://doi.org/10.1107/S0021889899006020.
[37] C.F. Macrae, P.R. Edgington, P. McCabe, E. Pidcock, G.P. Shields, R. Taylor, M. Towler, J. van de Streek, *Mercury*: visualization and analysis of crystal structures, J. Appl. Crystallogr 39 (2006) 453–457, https://doi.org/10.1107/S002188980600731X.
[38] A.L. Spek, Single-crystal structure validation with the program *PLATON*, J. Appl. Crystallogr 36 (2003) 7–13, https://doi.org/10.1107/S0021889802022112.
[39] G.M. Morris, R. Huey, W. Lindstrom, M.F. Sanner, R.K. Belew, D.S. Goodsell, A. J. Olson, AutoDock4 and AutoDockTools4: Automated docking with selective receptor flexibility, J. Comput. Chem. 30 (2009) 2785–2791, https://doi.org/10.1002/jcc.21256.
[40] O. Trott, A.J. Olson, AutoDock Vina: Improving the speed and accuracy of docking with a new scoring function, efficient optimization, and multithreading, J. Comput. Chem. (2009), https://doi.org/10.1002/jcc.21334.